

### SLC41A1 is a novel mammalian Mg<sup>2+</sup> carrier

Martin Kolisek<sup>1,3‡\*</sup>, Pierre Launay<sup>2‡\*</sup>, Andreas Beck<sup>3‡</sup>, Gerhard Sponder<sup>4</sup>, Nicolas Serafini<sup>2</sup>, Marcel Brenkus<sup>1</sup>, Elisabeth Maria Froschauer<sup>4</sup>, Holger Martens<sup>1</sup>, Andrea Fleig<sup>3\*</sup> and Monika Schweigel<sup>5\*</sup>

<sup>1</sup>Institute of Veterinary-Physiology, FU Berlin, Oertzenweg 19b, D-14163 Berlin, Germany

<sup>2</sup>INSERM, U699, Equipe Avenir, Paris, F-75018, France

<sup>3</sup>Laboratory of Cell and Molecular Signalling, Center for Biomedical Research at The Queen's Medical Center, 1301 Punchbowl St., UHT 8, HI 96813 Honolulu, USA

<sup>4</sup>Max F. Perutz Laboratories, Department of Microbiology and Genetics, University of Vienna, Dr. Bohrgasse 9, A-1030 Vienna, Austria

<sup>5</sup>Research Institute for the Biology of Farm Animals (FBN), Department of Nutritional Physiology "Oskar Kellner", Wilhelm-Stahl-Allee 2, D-18196 Dummerstorf, Germany

\* Corresponding authors; ‡ these authors contributed equally

[martink@zedat.fu-berlin.de](mailto:martink@zedat.fu-berlin.de) (tel: +49-30-83862628; fax: +49-30-83862610),  
[pierre.launay@bichat.inserm.fr](mailto:pierre.launay@bichat.inserm.fr), [afleig@hawaii.edu](mailto:afleig@hawaii.edu) or [mschweigel@fbn-dummerstorf.de](mailto:mschweigel@fbn-dummerstorf.de)

Running title: SLC41A1, a novel Mg<sup>2+</sup> carrier

The molecular biology of mammalian magnesium transporters and their interrelations in cellular magnesium homeostasis are largely unknown. Recently, the mouse SLC41A1 protein was suggested to be a candidate magnesium transporter with channel-like properties when over-expressed in *Xenopus laevis* oocytes. Here, we demonstrate that human SLC41A1 over-expressed in HEK293 cells forms protein complexes and locates to the plasma membrane without, however, giving rise to any detectable magnesium currents during whole-cell patch-clamp experiments. Nevertheless, in a strain of *Salmonella enterica* exhibiting disruption of all three distinct magnesium transport systems (CorA, MgtA and MgtB), over-expression of human SLC41A1 functionally substitutes these transporters and restores the growth of the mutant bacteria at magnesium concentrations otherwise non-permissive for growth. Thus, we have identified human SLC41A1 as being a *bona fide* magnesium transporter. Most importantly, over-expressed SLC41A1 provide HEK293 cells with an increased magnesium efflux capacity. With outwardly directed Mg<sup>2+</sup> gradients, a SLC41A1-dependent reduction of the free intracellular magnesium concentration accompanied by a significant net decrease of the total cellular magnesium concentration

could be observed in such cells. SLC41A1 activity is temperature-sensitive but not sensitive to the only known magnesium channel blocker, cobalt(III)hexaammine. Taken together, these data functionally identify SLC41A1 as a mammalian carrier mediating magnesium efflux.

Intracellular magnesium, especially its ionized fraction (Mg<sup>2+</sup>), plays a critical role in enzyme activation, making the ion essential for numerous metabolic processes (1). Mg<sup>2+</sup> is an important co-factor in a number of other physiological functions, including the synthesis of biomacromolecules, secretion of hormones and modulation of ion channel activity (2; 3). It is therefore not surprising that an abnormal Mg<sup>2+</sup> homeostasis is associated with several disease conditions, such as cardiovascular diseases, essential hypertension, diabetes mellitus, and metabolic syndrome (4; 5; 6). However, a better understanding of cellular Mg<sup>2+</sup> transport mechanisms and regulation is needed to elucidate the exact role of Mg<sup>2+</sup> in these disease processes; at present, this is hampered by limited knowledge of the molecular fundament of the mammalian Mg<sup>2+</sup> transport network. Despite extensive evidence for the existence of various regulated Mg<sup>2+</sup> transport proteins (7; 8; 9; 10), only two plasma-membrane localized proteins have been

identified at the molecular level, namely, TRPM6 and TRPM7, which are ion channels of the melastatin-related transient receptor potential family, and MRS2, a channel located in the inner mitochondrial membrane (11; 12; 13). Thus, the recent description of novel putative Mg<sup>2+</sup> transporters, such as the A1 and A2 members of the solute carrier family 41 (SLC41) (14; 15; 16; 17), the ancient conserved domain protein (ACDP) subtype 2 (18; 19), a protein termed magnesium transporter 1 (MagT1) (20) and the protein NIPA1 (21), have significantly expanded the field of research into cellular Mg<sup>2+</sup> transport systems.

The eukaryotic proteins SLC41A2 and SLC41A3, together with the protein SLC41A1, form a novel and unique family among the SLC superfamily, which contains 44 families of proteins involved in the transport of various inorganic and organic solutes (22; HUGO database). *SLC41A1* was first identified and bioinformatically described by Wabakken et al. (14). Human *SLC41A1* (*hSLC41A1*) has been mapped to chromosome 1q31-32 and encodes a protein consisting of 513 amino acids with a predicted molecular mass of 56 kDa (14). In humans and mice, the 5 kb long *SLC41A1* transcripts have been found in most tissues (notably in heart, muscle, testis, thyroid gland and kidney) (14; 15). Homologues of the *hSLC41A1* have also been identified in worms and insects.

A role of SLC41A1 in Mg<sup>2+</sup> cellular transport suggests itself because of its partial sequence homology to the bacterial Mg<sup>2+</sup> transporter MgtE (14; 23; 24). Experiments show that feeding mice on a low Mg<sup>2+</sup> diet causes increased expression of *SLC41A1* in the kidney, colon and heart (15). Moreover, analysis of published sequences has predicted SLC41A1 to be an integral cell membrane protein possessing 10 transmembrane domains (TM). However, the only direct experimental evidence for SLC41A1 being an Mg<sup>2+</sup> transporter has been reported by Goytain and Quamme (15). By using a two-electrode-voltage clamp (TEV), the authors suggest that heterologous expression of mouse *SLC41A1* (*mSLC41A1*) in *Xenopus laevis* oocytes induces large inward currents carried by Mg<sup>2+</sup>.

In this study, we have identified SLC41A1 as an eukaryotic Mg<sup>2+</sup> carrier with the ability to form protein complexes. We show that SLC41A1 mediates a slow temperature-sensitive transport of

Mg<sup>2+</sup> and, importantly, that it is able to substitute genetically distant bacterial Mg<sup>2+</sup> transporters CorA, MgtA and MgtB at a functional level in *Salmonella*. Overall, our data suggest that SLC41A1 is an Mg<sup>2+</sup> carrier playing a significant role in transmembrane Mg<sup>2+</sup> transport and, by extrapolation, in cellular Mg<sup>2+</sup> homeostasis.

## Experimental procedures

### *Salmonella enterica* sv. *typhimurium*

#### Strains, plasmids, growth media and cultivation conditions

Strain MM1927: DEL485(LeuBCD), mgtB::MudJ; mgtA21::MudJ; corA45::mudJ; zjh1628::Tn10(cam) Cam<sup>R</sup>, Kan<sup>R</sup>; *pALTER-corA* (Amp<sup>R</sup>)

Strain MM281: DEL485(LeuBCD), mgtB::MudJ; mgtA21::MudJ; corA45::mudJ; zjh1628::Tn10(cam) Cam<sup>R</sup>, Kan<sup>R</sup> (Mg<sup>2+</sup> dependent strain)

Strains MM1927 and MM281 were kindly provided by M. E. Maguire (Case Western Reserve University Cleveland USA).

Strain MM281-*pUC18-SLC41A1*: DEL485(LeuBCD), mgtB::MudJ; mgtA21::MudJ; corA45::mudJ; zjh1628::Tn10(cam) Cam<sup>R</sup>, Kan<sup>R</sup>; *pUC18-SLC41A1*.

*hSLC41A1* was amplified by the polymerase chain reaction (PCR) from the point-mutation-corrected plasmid *pGEM-T-hSLC41A1* (the original plasmid was provided by H-C. Aasheim, Radium Hospital Oslo, Norway) by using specific primers SLC1-1-6xHis-XbaI

5'-tgcTCTAGAatgCATCACCATCACCATCACTcctctaagccagag-3' and SLC2-1-HindIII 5'-cccAAGCTTctagtccccgacatcc-3' and cloned into plasmid *pUC18*. The *pUC18-hSLC41A1* and *pUC18-(empty)* isolated from *E. coli* were transfected into *Salmonella* transmitter strain LT2-LB5010 (*str<sup>R</sup>*, r<sup>-</sup>, m<sup>+</sup>) (25). If not otherwise stated, *hSLC41A1* expression was induced by addition of 0.05 mmol.l<sup>-1</sup> isopropyl-β-D-thiogalactopyranosid (IPTG) to the growth media.

LB medium containing 10 mmol.l<sup>-1</sup> MgCl<sub>2</sub> was used to culture the MM281 strain. The solid and liquid N-minimal media for complementation tests were prepared according to Nelson and Kennedy (26), except that 0.5 mmol.l<sup>-1</sup> Na<sub>2</sub>SO<sub>4</sub> was used

instead of 0.5 mmol.l<sup>-1</sup> K<sub>2</sub>SO<sub>4</sub>. In addition, the media were supplemented with 0.1% casamino acids (DIFCO BD) and thiamine (2 mg.l<sup>-1</sup>, Sigma). Over-night cultures grown in LB medium (37°C, provided with Mg<sup>2+</sup> if necessary) were washed with 0.7% saline, adjusted to an OD<sub>600</sub> of 0.1 and diluted as indicated in fig. 4. Serial dilutions were spotted onto N-minimal medium plates containing 10 mmol.l<sup>-1</sup>, 100 μmol.l<sup>-1</sup> or 10 μmol.l<sup>-1</sup> MgCl<sub>2</sub>. Spotted bacteria were cultivated for 36 hrs. To establish growth curves, over-night cultures grown in LB medium were washed with 0.7% saline, adjusted to an OD<sub>600</sub> of 0.1 and inoculated into liquid N-minimal media containing 10 mmol.l<sup>-1</sup>, 100 μmol.l<sup>-1</sup> or 10 μmol.l<sup>-1</sup> MgCl<sub>2</sub>.

#### *Immuno-precipitation and Western blot analysis*

Total proteins were extracted from 250 ml of the bacterial culture (-IPTG or +IPTG, as indicated) using TCA/acetone. Proteins of the membrane fraction were isolated using ProteoExtract™ Partial Bacterial Proteome Extraction Kit (Calbiochem La Jolla USA). His-tagged hSLC41A1 was immuno-precipitated from the membrane protein fraction with a 6x His-tag antibody (GenWay Biotech San Diego USA). Protein samples were separated by SDS-PAGE utilizing 12.5% polyacrylamide gels, blotted and labelled with 6x His-tag antibody and goat anti-mouse (GAM)-HRP (Molecular Probes Eugene USA) or GAM-kappa-HRP (SBA Birmingham USA) antibodies. Antibody binding was visualised using the Chemilmager™ 5500 (Alpha Innotech USA) or AGFA Cronex 5 mediocal x-ray films developed with the Curix 60 (AGFA).

#### *Determination of total Mg in Salmonella by ICP-Mass Spectroscopy (ICP-MS)*

Cultures of strains MM1927, MM281 and MM281-pUC18-hSLC41A1, grown (24 hrs) in N-minimal medium supplemented with 2 mmol.l<sup>-1</sup> or 10 mmol.l<sup>-1</sup> Mg<sup>2+</sup>, were washed 3 times with 0.7% saline and diluted to a bacterial density of 3 x 10<sup>8</sup> bacteria.ml<sup>-1</sup>. Diluted bacterial suspensions (1 ml each) were centrifuged. Dried bacterial pellets were resuspended in 0.3 ml 1 N HNO<sub>3</sub> and 0.7 ml of 1-bromododecane (*purum-purum*, Roth Karlsruhe Germany). Samples were centrifuged and the upper water fractions were used to determine total Mg contents (ICP-MS ELAN

6100, Perkin-Elmer). The organic fractions were used to determine protein contents.

#### *Determination of free intracellular Mg<sup>2+</sup> in Salmonella by mag-fura 2 FF-Spectrofluorometry*

Experimental procedures and data analyses were conducted according to Froschauer et al. (27) except the mag-fura 2 AM loading facilitator Pluronic F-127 was used at a final concentration of 5 μmol.l<sup>-1</sup> and the mag-fura 2 AM loading period was 30 mins. Measurements were performed with a spectrofluorometer LS-55, operated by software FL WinLab vers. 4.0 (both products of Perkin-Elmer) at 37°C, in 3 ml cuvettes containing bacterial suspension (2 ml, 3 x 10<sup>8</sup> bacteria.ml<sup>-1</sup>).

#### *HEK293- and HEK293-derived cell lines*

##### *Growth media and culture conditions*

HEK293-(FLAG-SLC41A1): Full-length hSLC41A1 cDNA was cloned into a modified version of the *pCDNA4/TO* vector (Invitrogen Carlsbad USA) with an N-terminal FLAG-tag. The *FLAG-hSLC41A1* cDNA in *pCDNA4/TO* was electroporated into HEK293 cells previously transfected with the *pCDNA6/TR* construct for Tet-repressor expression. Cells were placed under zeocin selection; zeocin-resistant clones were screened for tet-inducible expression of the FLAG-tagged hSLC41A1 protein.

Tet-inducible HEK293-(FLAG-SLC41A1) cells were cultured in DMEM (Biochrom AG Berlin Germany) containing 10% fetal bovine serum (FBS, PAN Biotech Aidenbach Germany), 2 mmol.l<sup>-1</sup> glutamine (PAN Biotech), PenStrep (PAN Biotech), Normocin™ (0.1 mg.ml<sup>-1</sup>, Cayla Toulouse France), blasticidin (5 μg.ml<sup>-1</sup>, Cayla) and zeocin (0.4 mg.ml<sup>-1</sup>, Cayla). *FLAG-SLC41A1* over-expression was induced with tetracycline (1 μg.ml<sup>-1</sup>, Fluka Germany).

HEK293-(HA-TRPM7): Cultivation conditions were as described in Schmitz et al. (12).

HEK293: Cells were cultured in DMEM medium supplemented with 10% FBS, 2 mmol.l<sup>-1</sup> glutamine, PenStrep and Normocin.

##### *Immuno-precipitation and Western blot analysis*

Non-induced (-tet) and induced (+tet, 15-18 hrs) HEK293-(FLAG-SLC41A1) cells (10<sup>7</sup> cells.ml<sup>-1</sup>) were lysed for 30 mins at 4°C in Tris buffer (pH 7.5) containing 1% Triton X-100 (Bio-Rad

Hercules USA) and protease inhibitors. Membrane protein fraction was isolated from the same cell types with ProteoExtract™ Native Membrane Protein Extraction Kit (M-PEK, Calbiochem). Both, total lysate proteins and membrane fraction proteins had been resolved by 10% SDS-PAGE, transferred to PVDF membranes and immunodecorated with anti-FLAG antibody coupled to HRP (Invitrogen), or with antibody to  $\beta$ -actin (AbCam Cambridge UK) conjugated to GAM HRP-linked antibody (Jackson ImmunoResearch Laboratories West Grove USA).

The same samples were immuno-precipitated by M2 anti-FLAG (Sigma) or isotype control, resolved by 10% SDS-PAGE and transferred to PVDF membranes. The membrane was immunoblotted with M2 anti-FLAG (Sigma) and GAM-kappa-HRP (SBA Birmingham USA). Membranes were developed by enhanced chemical luminescence (ECL) (Amersham Pharmacia Biotech).

#### *Blue-native polyacrylamide gel electrophoretic (BN-PAGE) separation and 2D-SDS-PAGE*

Enriched native membrane proteins were isolated from +tet (15 hrs) HEK293-(SLC41A1) cells by use of the ProteoExtract™ M-PEK. Native protein samples were mixed with SDS and incubated for 10 mins in a thermomixer at 37°C with moderate shaking before being separated on the BN-polyacrylamide gel gradient (4% > 12%) according to the protocol of Swamy et al. (28). Proteins forming complexes with SLC41A1 were resolved by 10% SDS-2D-PAGE and stained with Silver Stain Plus (Bio-Rad). The 2D-gels running in parallel with those used for silver staining were blotted and immuno-decorated with M2 anti-FLAG and GAM HRP-linked antibodies and FLAG-SLC41A1 was visualized by a Chemilmager™ 5500 (Alpha Innotech). Protein marker Native Mark™ was purchased from Invitrogen.

#### *Confocal Microscopy*

$5 \times 10^5$  HEK293-(FLAG-SLC41A1) cells were plated on 12 mm glass, gelatine (2%) coated coverslips and cultured for 24 hrs. Thereafter, FLAG-hSLC-41A1 over-expression was induced with tetracycline (15 hrs). Then, labeling of +tet and -tet cells with Alexa Fluor-594 wheat germ agglutinin ( $2 \mu\text{g}\cdot\text{ml}^{-1}$ , 10 mins at 4°C) purchased

from Invitrogen was performed. After rinsing with PBS, cells were fixed in 100% methanol (10 mins at -20°C). All following steps were carried out at room temperature. Cells were rinsed with PBS, blocked for 1h in PBS containing 0.5% FSG (Sigma) and then rinsed with PBS containing 0.02% FSG. Subsequently, they were incubated for 45 mins each with the primary M2 anti-FLAG antibody ( $1 \text{ mg}\cdot\text{ml}^{-1}$ ) and with the secondary GAM-antibody ( $0.4 \text{ mg}\cdot\text{ml}^{-1}$ , Invitrogen) labeled with Alexa Fluor-488. Processed samples were coated with 5  $\mu\text{l}$  of vectoshield (Vector Laboratories, Burlingame USA) and digital images were acquired using a confocal microscope Zeiss LSM 510 META (Zeiss Jena Germany). Colocalization correlation analysis was performed using Zeiss LSM 510 Image Browser (Zeiss).

#### *Electrophysiology*

Whole-cell-mode patch-clamp experiments were performed at 21 - 25°C. Data were acquired with Pulse software controlling an EPC-9 amplifier (HEKA Lambrecht/Pfalz Germany) with settings as described in Schmitz et al. (12). Coverslip-grown -tet and +tet HEK293-(SLC41A1) and HEK293-(TRPM7) cells were kept, during all experiments, in Ringer's solution of the following composition (in  $\text{mmol}\cdot\text{l}^{-1}$ ): NaCl 140, KCl 2.8, CaCl<sub>2</sub> 1, MgCl<sub>2</sub> 2, HEPES 10, glucose 10, the pH being adjusted to 7.2 with NaOH. SLC41A1 intracellular pipette-filling buffer contained (in  $\text{mmol}\cdot\text{l}^{-1}$ ): K<sup>+</sup>Glu 140, NaCl 8, HEPES 10, the pH being adjusted to 7.2 with NaOH. TRPM7 intracellular pipette-filling buffer contained (in  $\text{mmol}\cdot\text{l}^{-1}$ ): Cs<sup>+</sup>Glu 140, NaCl 8, HEPES 10, Cs<sup>+</sup>BAPTA 10, the pH being adjusted to 7.2 with CsOH. In one series of experiments, a low Cl<sup>-</sup> Ringer's solution (in  $\text{mmol}\cdot\text{l}^{-1}$ : Na-Glutamate 140, KCl 2.8, CaCl<sub>2</sub> 1, MgCl<sub>2</sub> 2, HEPES 10, glucose 10, pH 7.2) was applied externally and cells were perfused with KCl-based SLC41A1 intracellular pipette-filling buffer (containing in  $\text{mmol}\cdot\text{l}^{-1}$ : KCl 140 instead of K<sup>+</sup>Glu 140).

The final osmolarity of each of the above buffers was ~300 mOsm.

#### *Determination of free intracellular Mg<sup>2+</sup> in +tet and -tet HEK293-(SLC41A1) cells by mag-fura 2 FF-Spectrofluorometry*

The -tet and +tet HEK293-(SLC41A1) cells were rinsed twice with ice-cold, completely divalent-free phosphate-buffered saline (PBS), detached by use of Hytase (Perbio Science Bonn Germany), centrifuged, washed twice in PBS and finally resuspended in completely Ca<sup>2+</sup>- and Mg<sup>2+</sup>-free Hank's balanced solution (CMF-HBS, pH 7.4, PAN Biotech). Loading of cells with 7.5 μmol.l<sup>-1</sup> mag-fura 2 AM (Molecular Probes) was performed for 25 mins at 37°C in the presence of pluronic acid. After being washed in CMF-HBS, cells were incubated for a further 30 mins to allow for complete de-esterification of the fluorescence probe, washed twice in CMF-HBS to remove extracellular mag-fura 2 and stored in CMF-HBS complemented with 10 mmol.l<sup>-1</sup> HEPES and 5 mmol.l<sup>-1</sup> glucose (CMF-HBS+) until used for measurements of free intracellular [Mg<sup>2+</sup>]<sub>i</sub> ([Mg<sup>2+</sup>]<sub>i</sub>). Measurements were made at 37°C (or as indicated in the results section) in 3 ml cuvettes containing cell suspension (2 ml, CMF-HBS+ with a cytocrit of 10%) under stirring after the cells had been washed twice in CMF-HBS+. In experiments with inside-directed Mg<sup>2+</sup> gradients, MgCl<sub>2</sub> was added to give final concentrations of 2, 5 or 10 mmol.l<sup>-1</sup> (30 to 40 s prior to start of the measurements). In control measurements, no Mg<sup>2+</sup> was added but, instead, 2, 5 or 10 mmol.l<sup>-1</sup> Ca<sup>2+</sup> was present in the measuring solution. [Mg<sup>2+</sup>]<sub>i</sub> was determined by measuring the fluorescence of the probe-loaded cells in a spectrofluorometer (LS50-B, Perkin-Elmer) by using the fast filter accessory, which allowed fluorescence to be measured at 20-ms intervals with excitation at 340 and 380 nm, and emission at 515 nm. [Mg<sup>2+</sup>]<sub>i</sub> values were calculated from the 340/380-nm ratio according to the formula of Grynkiewicz et al. (29) by using the software FL WinLab version 4.0 (Perkin-Elmer). A dissociation constant of 1.5 mmol.l<sup>-1</sup> for the mag-fura 2/Mg<sup>2+</sup> complex was used for calculations; minimum (R<sub>min</sub>) and maximum (R<sub>max</sub>) ratios were determined at the end of each experiment by using digitonin. R<sub>max</sub> was found by the addition of 25 mmol.l<sup>-1</sup> MgCl<sub>2</sub> in the absence of Ca<sup>2+</sup>, whereas R<sub>min</sub> was obtained by addition of 50 mmol.l<sup>-1</sup> EDTA, pH 7.2, to remove all Mg<sup>2+</sup> from the solution. For data evaluation, 10-second data sets each were averaged at the beginning of the measurement and then always after 50 seconds. The final [Mg<sup>2+</sup>]<sub>i</sub> was determined as the mean [Mg<sup>2+</sup>]<sub>i</sub> of the last 10 seconds of the

measurement. Thus, for the calculation of any given [Mg<sup>2+</sup>]<sub>i</sub>, 500 data points were used. If not otherwise stated, data are presented as means ± standard error (SE).

#### *Determination of free intracellular Ca<sup>2+</sup> in +tet and -tet HEK293-(SLC41A1) cells by fura 2 FF-Spectrofluorometry*

The general procedure was the same as that described for the determination of [Mg<sup>2+</sup>]<sub>i</sub> with the following exceptions. Cells were loaded with 10 μmol.l<sup>-1</sup> fura 2 AM. The R<sub>max</sub> for fura 2 was obtained in solutions with 2 mM Ca<sup>2+</sup> and the R<sub>min</sub> by the addition of 20 mmol.l<sup>-1</sup> EGTA, pH 8.0; a dissociation constant of 224 nmol.l<sup>-1</sup> was used for the fura 2/Ca<sup>2+</sup> complex.

#### *Determination of the total Mg in -tet and +tet (15 hrs) HEK293-(FLAG-SLC41A1) by atomic mass spectroscopy (AMS)*

The -tet and +tet (15 hrs) HEK293-(FLAG-SLC41A1) cells were grown to ~80% confluency, washed twice with serum-free, Mg<sup>2+</sup>/Ca<sup>2+</sup>-free HEK293 experimental medium (PAN Biotech), detached by 0.25% trypsin-EDTA buffer and resuspended in HEK293 medium to give a final cell count of 6 x 10<sup>6</sup> cells.ml<sup>-1</sup>. The viability of the cells was determined by using Trypan Blue exclusion. Diluted cells were held in the synthetic HEK293 medium for 60 mins prior to the addition of Mg<sup>2+</sup> to give a final [Mg<sup>2+</sup>]<sub>e</sub> of 10 mmol.l<sup>-1</sup>. Subsequently, the cells were incubated in the presence of Mg<sup>2+</sup> at 37°C in 5% CO<sub>2</sub> atmosphere for 20 or 180 mins. After incubation, they were washed three times with Mg<sup>2+</sup>/Ca<sup>2+</sup>-free PBS and dried pellets were mixed with 0.3 ml 1 N HNO<sub>3</sub> and 0.7 ml 1-bromododecane (*purum-purum*). Samples were centrifuged and the upper water fractions were used to determine total Mg contents (flame AM Spectrometer M Series, Thermo Scientific USA). Protein contents were determined in the organic fractions.

#### *Statistics*

All statistical calculations were performed by using SigmaStat (Jandel Scientific). Significance was determined by *Students t*-test; *P* < 0.05 was considered to be significant.

#### *Inhibitors*

DIDS and cobalt(III)hexaammine (CoHex) were obtained from Sigma. H<sub>2</sub>DIDS was purchased from Molecular Probes.

## Results

To assess the basic molecular characteristics of SLC41A1 and its role in cellular Mg<sup>2+</sup> transport, we took advantage of the well-established tetracycline-controlled expression system in the HEK293 cell line. Several zeocin resistant clones were tested; clone 17 was selected for this study, because of the high level of over-expression and the lack of molecular leakiness (figs. 1B and 1C).

*Cell topography of recombinant FLAG-hSLC41A1*  
Computational analyses predicted SLC41A1 to be an integral cell membrane protein with 10 putative transmembrane domains (TM) and possibly both N- and C-termini located intracellularly (fig. 1A) (14; 15; PSORT II and WOLF PSORT II Prediction). To test whether over-expressed *FLAG-hSLC41A1* was targeted to the plasma membrane of the HEK293 cells, we designed several experiments comprising confocal immunolocalization and Western blot analysis of the membrane protein fraction isolated from non-induced (-tet) and tet-induced (+tet) HEK293-(FLAG-hSLC41A1).

As shown in figure 1B, the recombinant FLAG-tagged SLC41A1 protein was specifically detected in the plasma membrane of +tet (15 hrs) HEK293-(FLAG-hSLC41A1) cells investigated by confocal microscopy. This was confirmed by colocalization of the green fluorescent signal of immuno-labelled hSLC41A1 (M2 anti-FLAG : GAM Alexa-488) with the red fluorescent signal of wheat germ agglutinin conjugated to Alexa-594 (fig. 1B). The latter is known to recognize sialic acid and N-acetylglucosaminyl sugar residues predominantly found on the plasma membrane. Colocalization correlation analysis revealed a  $59.3 \pm 1.6\%$  overlap of red and green pixels (Sfs. 1A, 1B and 1C). In contrast, no FLAG-hSLC41A1-specific fluorescence was found in -tet cells (fig. 1B). Figure 1C shows data obtained by Western blot analysis of membrane protein fractions (MF) and of non-membrane protein fractions (NMF) from -tet and +tet (18 hrs) cells. The 56-kDa band corresponding to FLAG-hSLC41A1 was predominantly detected in the MF with lower

abundance in NMF. Western blot analysis of immuno-precipitated FLAG-hSLC41A1 from MF and NMF lysates revealed the same results (fig. 1C). FLAG-hSLC41A1-specific band was not detected in samples prepared from -tet cells. Taken together, these data demonstrate the plasma membrane localization of FLAG-hSLC41A1 when over-expressed in HEK293 cells (fig. 1A).

### *Complex forming ability of hSLC41A1*

Various solute transporters have been shown to form stable or transient protein complexes, which are necessary in order for them to be functional (31; 32). To test whether hSLC41A1 formed such complexes with other proteins, we performed BN-PAGE with native proteins isolated from +tet (15 hrs) HEK293-(SLC41A1) cells. FLAG-hSLC41A1-containing complexes were immuno-detected with M2 anti-FLAG and goat anti-mouse HRP-linked antibodies. We identified two complexes (C1, C2; fig. 2A) with molecular masses lying between 720 kDa and 1236 kDa (720 kDa < C1, C2 < 1236 kDa). Next, the hSLC41A1 complexes were gradually degraded by adding SDS in a stepwise manner to give concentrations from 0.05% to 1%. Upon addition of 0.1% SDS, we were able to detect the break-down products of C1 and C2: 480 kDa < C3 < 720 kDa; 242 kDa < C4 < 480 kDa and M ~56 kDa, the latter corresponding to the molecular mass of the SLC41A1 monomer (fig. 2A). A successive increase of SDS strengthened the signal of C4 and of M and, as expected, weakened the signal of C1 and C2. The 2D-SDS-PAGE separation of the C1 and C2 complexes followed by silver staining revealed heterogeneous compositions of C1 and C2 complexes (data not shown). Because of the limited resolution of the high molecular mass protein complexes (750 kDa << C<sub>x</sub>) in the first native dimension, the presence of SLC41A1 in C1 and C2 complexes was confirmed by SLC41A1 immuno-decoration after 2D-SDS-PAGE (fig. 2B).

### *Effect of hSLC41A1 over-expression on growth and Mg<sup>2+</sup> content of Mg<sup>2+</sup>-deficient Salmonella strain MM281*

The *hSLC41A1* gene shares sequence similarity with the bacterial gene *mgtE* (14; 15). Gene *mgtE* has been identified in various bacteria (23; 24), but not in *Salmonella sp.* Based on its ability to restore

growth of the Mg<sup>2+</sup>-deficient strain MM281 of *Salmonella enterica*, Smith and colleagues (24) have proposed the direct involvement of MgtE in Mg<sup>2+</sup> transport. Strain MM281 exhibits disruption of genes *corA*, *mgtA* and *mgtB*, the three major Mg<sup>2+</sup> influx systems of *Salmonella*. Compared with normal strains that can grow at [Mg<sup>2+</sup>]<sub>e</sub> of 10 to 100 μmol.l<sup>-1</sup>, this strain requires [Mg<sup>2+</sup>]<sub>e</sub> from 10 to 100 mmol.l<sup>-1</sup> to proliferate (24; 28).

We tested the ability of hSLC41A1 to complement the Mg<sup>2+</sup>-dependent growth-deficient phenotype of strain MM281 by transforming it with the plasmid *pUC18-hSLC41A1* or *pUC18-(empty)*.

The expression of His-hSLC41A1 after addition of IPTG (0.02 to 0.05 mmol.l<sup>-1</sup>) was confirmed by Western blot analysis of the total protein isolate as well as of the immuno-precipitated His-hSLC41A1 from the bacterial membrane protein fraction (fig. 3). Growth curves were established within 24 hrs for strains MM281-*pUC18-(empty)*, MM281-*pUC18-hSLC41A1* and MM1927, in media containing 10 μmol.l<sup>-1</sup>, 100 μmol.l<sup>-1</sup> or 10 mmol.l<sup>-1</sup> Mg<sup>2+</sup>. The growth maxima of strains MM1927 and MM281-*pUC18-hSLC41A1* were almost identical at [Mg<sup>2+</sup>]<sub>e</sub> of 10 mmol.l<sup>-1</sup>, whereas the growth maximum of strain MM281-*pUC18-(empty)* was approximately 33% lower in comparison with the growth maximum of strain MM1927 (fig. 4A). The growth maximum of strain MM281-*pUC18-hSLC41A1* reached 43% of the growth maximum of strain MM1927 when cultivated at an [Mg<sup>2+</sup>]<sub>e</sub> of 100 μmol.l<sup>-1</sup> (fig. 4B) and 32.5% when cultivated at an [Mg<sup>2+</sup>]<sub>e</sub> of 10 μmol.l<sup>-1</sup> (fig. 4C). Strain MM281-*pUC18-(empty)* did not grow in media supplemented with an [Mg<sup>2+</sup>]<sub>e</sub> of 10 μmol.l<sup>-1</sup> or 100 μmol.l<sup>-1</sup>. As shown in fig. 4, images of the plated serial dilutions obtained after 24 hrs of incubation at 37°C clearly corresponded to the respective sets of the growth curves.

Further we measured the [Mg<sup>2+</sup>]<sub>i</sub> of bacteria from strains MM1927, MM281-*pUC18-(empty)* and MM281-*pUC18-hSLC41A1* by using mag-fura 2 fast filter spectroscopy (FFS) (27). Mg<sup>2+</sup>-starved bacteria were incubated in 0.9% saline containing 0 or 10 mmol.l<sup>-1</sup> Mg<sup>2+</sup> and the [Mg<sup>2+</sup>]<sub>i</sub> was determined over 20 mins. The results are summarized in figure 4D. The basal [Mg<sup>2+</sup>]<sub>i</sub> measured in Mg<sup>2+</sup>-free solution was 0.91 ± 0.04, 0.93 ± 0.07 and 0.87 ± 0.03 mmol.l<sup>-1</sup> in MM1927, MM281-*pUC18-(empty)* and MM281-*pUC18-*

*hSLC41A1* bacteria, respectively. In MM1927 and MM281-*pUC18-hSLC41A1* bacteria an 89.5% and 42.2% increase of [Mg<sup>2+</sup>]<sub>i</sub> was observed after increasing the [Mg<sup>2+</sup>]<sub>e</sub> of the external solution to 10 mmol.l<sup>-1</sup>. In contrast, no change of [Mg<sup>2+</sup>]<sub>i</sub> was measured in strain MM281-*pUC18-(empty)*.

The mag-fura 2 data are in agreement with our results obtained by using ICP-MS. With this technique, the relative increase of the total Mg concentration (Δ[Mg]<sub>t</sub>) for bacteria grown 24 hrs at an [Mg<sup>2+</sup>]<sub>e</sub> of 2 mmol.l<sup>-1</sup> and those grown at an [Mg<sup>2+</sup>]<sub>e</sub> of 10 mmol.l<sup>-1</sup> was established for all three strains. The Δ[Mg]<sub>t</sub> for MM281-*pUC18-hSLC41A1* was 14.2%, similar to the 16.7% Δ[Mg]<sub>t</sub> measured in MM1927. The Δ[Mg]<sub>t</sub>(MM281-*pUC18-(empty)*) remained at 7.3% and was significantly less than the Δ[Mg]<sub>t</sub> determined for strains MM1927 and MM281-*pUC18-hSLC41A1*.

#### Patch-clamp characterization of hSLC41A1

Using TEV, Goytain and Quamme (15) observed large Mg<sup>2+</sup> currents associated with mouse SLC41A1 when over-expressed in *Xenopus laevis* oocytes. Therefore, we expected Mg<sup>2+</sup> carried currents to appear after hSLC41A1 over-expression in HEK293 cells. In order to characterize such currents, patch-clamp experiments in the whole-cell configuration with +tet (15-18 hrs) and non-induced HEK293-(SLC41A1) cells were performed. Repetitive voltage ramps that spanned -100 to +100 mV over 50 ms were delivered every 2 s from a holding potential of 0 mV. Inward currents were assessed at -80 mV and outward currents at +80 mV. An inwardly directed Mg<sup>2+</sup> concentration gradient was created by perfusion of cells with Mg<sup>2+</sup>-free internal saline (K<sup>+</sup>Glu-based, if not stated otherwise), whereas the external solution contained 2 mmol.l<sup>-1</sup> Mg<sup>2+</sup>. Under these experimental conditions, development of a small but identifiable current at negative membrane potentials (-100 mV to 0 mV) would be predicted in SLC41A1 over-expressing cells that would not be seen in non-induced cells. This current would be expected to have a more positive reversal potential (E<sub>rev</sub>) and would be carried by Mg<sup>2+</sup>. Instead, SLC41A1 over-expressing cells developed a large outwardly rectifying conductance (fig. 5A). This current was fully activated within 200 s of the experiment and its

current-voltage (I-V) relationship (fig. 5B) revealed a highly nonlinear current with a reversal potential of around -35 mV. The development of the SLC41A1-induced current could be prevented in the presence of 1 mmol.l<sup>-1</sup> intracellular Mg<sup>2+</sup> (figs. 5C and 5D).

To test whether the SLC41A1-induced conductance could support Mg<sup>2+</sup> influx, cells were initially bathed in the standard external solution containing 1 mmol.l<sup>-1</sup> Ca<sup>2+</sup> and 2 mmol.l<sup>-1</sup> Mg<sup>2+</sup>. At 200 s, when the SLC41A1-induced conductance had reached its full amplitude, an isotonic solution of 115 mmol.l<sup>-1</sup> Mg<sup>2+</sup> was applied for 60 s via a buffer pipette (fig. 5E). This had no significant effect on either inward or outward currents, and the shape of the I-V relationship extracted at the end of application was also not affected compared with the control (data not shown). In conclusion these unexpected results clearly show that the SLC41A1-induced conductance did not give rise to an Mg<sup>2+</sup> influx but exhibited typical characteristics of a chloride conductance.

Therefore, further experiments were set out to confirm the latter. To this end, we allowed the current to develop fully before applying an external solution supplemented with 100 μmol.l<sup>-1</sup> of the Cl<sup>-</sup> channel inhibitor DIDS. This resulted in a fast and almost complete block of the current (figs. 5F, G). In control experiments with +tet (15-18 hrs) HEK293-(TRPM7) cells, the application of 100 μmol.l<sup>-1</sup> DIDS had no effect on TRPM7 current (Sf. 2).

In the next set of experiments we used Mg<sup>2+</sup>-free KCl-based instead of K<sup>+</sup>Glu-based internal saline. Under these conditions we observed: (1) an inward current which could not be seen when K<sup>+</sup>Glu buffer was used for perfusion of +tet HEK293-(SLC41A1) cells (Sfs. 3A and 3B) and (2) a depolarizing shift of the E<sub>rev</sub> as predicted for Cl<sup>-</sup> conductance by Nernst equation (Sf. 3B). At 300 s, a low Cl<sup>-</sup> solution was applied for 100 s via a buffer pipette. As expected, this resulted in a strong reduction of the outward current during application while the inward current remained the same (Sf. 3A). The application of low Cl<sup>-</sup> solution also evoked a further depolarizing shift of the E<sub>rev</sub> (Sf. 3B). These data in conjunction with the DIDS sensitivity of the current clearly confirm the involvement of Cl<sup>-</sup> channels.

Since some Cl<sup>-</sup> channels are activated by protein phosphorylation (33; 34) we wished to determine whether the SLC41A1-induced conductance would also be activated. To this end, we perfused both -tet and +tet cells with a Mg<sup>2+</sup>-free intracellular solution supplemented with 1 mmol.l<sup>-1</sup> ATPγS, a non-hydrolysable substrate for ATPases. In -tet cells, ATPγS gave rise to a Cl<sup>-</sup> conductance that was identical to the conductance and I-V curves seen in +tet cells in the absence of this substrate (fig. 5H). Moreover, ATPγS did not cause recruitment of any additional currents in SLC41A1-overexpressing cells (fig. 5A versus 5H and 5I) and the ATPγS-induced currents developed in an identical manner even in the complete absence of intracellular and extracellular Mg<sup>2+</sup> (data not shown). We wondered whether suppression of the SLC41A1-induced Cl<sup>-</sup> conductance would reveal any Mg<sup>2+</sup> influx that might have been masked by the large currents that develop in +tet cells. However, upon suppression of the Cl<sup>-</sup> currents by supplementing the extracellular solution with 100 μmol.l<sup>-1</sup> DIDS and superfusing the cells with an isotonic Mg<sup>2+</sup> solution, no further Mg<sup>2+</sup> influx could be detected (fig. 5J).

It is known that two molecules of tetracycline can chelate one Mg<sup>2+</sup> (30). To exclude any tetracycline effects on our measurements, wild type (wt) HEK293 cells grown for 15 hrs in tetracycline-containing medium (1 μg/ml) were perfused with Mg<sup>2+</sup>-free internal saline and examined in whole cell mode patch clamp experiments. As predicted no conductance similar to that measured in SLC41A1 over-expressing HEK293 cells was found in wt cells grown in +tet-medium (Sf. 4).

#### *Functional characterization of hSLC41A1 in HEK293 cells by use of mag-fura 2*

Because of the sequence homology of SLC41A1 to the bacterial Mg<sup>2+</sup> transporter MgtE, we wondered whether this protein might be involved in Mg<sup>2+</sup> transport functioning as a carrier protein rather than an ion channel mechanism. We therefore set out to measure intracellular Mg<sup>2+</sup> concentrations by using a mag-fura 2-based ratiometric assay. HEK293 cells bearing FLAG-tagged SLC41A1 were induced for 5, 10 or 15 hrs with tetracycline and, afterwards, the [Mg<sup>2+</sup>]<sub>i</sub> was measured over a 20-mins period in media with an

$[Mg^{2+}]_e$  of 0, 2, 5 or 10  $mmol.l^{-1}$ . The -tet HEK293-(SLC41A1) cells were used in control experiments. Representative original recordings of  $[Mg^{2+}]_i$  measurements in +tet (15 hrs) and -tet cells are shown in fig. 6A. In table I,  $[Mg^{2+}]_i$  values determined at the end of the measuring period are summarized for all conditions.

The incubation of +tet HEK293-(SLC41A1) cells in completely  $Mg^{2+}$ -free medium always led to a significant decrease of their  $[Mg^{2+}]_i$  compared with that of -tet HEK293-(SLC41A1) cells (figs. 6A and 6B, tab. I). The lower end point  $[Mg^{2+}]_i$  of +tet HEK293-(SLC41A1) cells resulted from a continuous decrease of their  $[Mg^{2+}]_i$  during the measuring period, amounting to  $41 \pm 8$ ,  $124 \pm 38$  and  $149 \pm 18 \mu mol.l^{-1}$  per 20 mins after 5, 10 and 15 hours of induction, respectively (fig. 6B). Such a process was never seen in -tet HEK293-(SLC41A1) cells or wild type HEK293 cells, which showed a negligible ( $56 \pm 7 \mu mol.l^{-1}$ )  $[Mg^{2+}]_i$  increase under these conditions. These surprising results point to an increased efflux capacity of HEK293 cells over-expressing SLC41A1.

Compared with the zero- $Mg^{2+}$  conditions, higher  $[Mg^{2+}]_i$  values were observed in both +tet and -tet cells if they were incubated in  $Mg^{2+}$ -containing medium (fig. 6A; tab. I). However, from 10 hrs and more after induction, +tet HEK293-(SLC41A1) cells had a significantly higher  $[Mg^{2+}]_i$  at the end of the measuring period than -tet cells at all  $[Mg^{2+}]_e$  used (tab. I). In contrast, no  $[Mg^{2+}]_i$  increase was observable in the presence of transmembrane  $Ca^{2+}$  gradients favoring calcium influx (fig. 6A). Control measurements performed by use of fura 2 showed that hSLC41A1 over-expression and/or increasing the extracellular  $[Ca^{2+}]$  from 2 to 10  $mmol.l^{-1}$  induced no elevation of the free cytosolic  $[Ca^{2+}]$  ( $[Ca^{2+}]_i$ ). The mean  $[Ca^{2+}]_i$  determined at the end of the measuring period always amounted to  $128 \pm 4 nmol.l^{-1}$ . Again, a possible effect of tetracycline-traces on the  $[Mg^{2+}]_i$  changes was tested in +tet (10 and 15 hrs) HEK293 wt cells. The results are summarized in table I showing that the  $[Mg^{2+}]_i$  of -tet or +tet wt HEK293 cells was not different from that measured in -tet HEK293-(SLC41A1) cells.

Since the patch-clamp data revealed an inhibition of the SLC41A1-related  $Cl^-$  conductance in +tet HEK293-(SLC41A1) cells treated with 100  $\mu mol.l^{-1}$  DIDS (fig. 5F, G), we investigated

whether this inhibitor also influenced their  $[Mg^{2+}]_i$ . As shown in figure 6C, this was not the case and the  $[Mg^{2+}]_i$  of +tet cells treated with the non-fluorescent  $H_2$ -DIDS (100  $\mu mol.l^{-1}$ ) was not different from that of untreated control cells.

In -tet HEK293-(SLC41A1) cells, the  $[Mg]_i$  increase was solely dependent on the extracellular  $[Mg^{2+}]$  in a linear ( $\Delta[Mg^{2+}] = 187.8 + 94.5[Mg^{2+}]_e$ ;  $r^2 = 0.99$ ) manner (fig. 6D). After correction for this linear component, a  $[Mg^{2+}]_i$  elevation was still observable in +tet HEK293-(SLC41A1) cells (fig. 6E). This remaining component was assumed to result mainly from SLC41A1 over-expression and its extent was dependent on  $[Mg^{2+}]_e$  and on the duration of tet-induction (fig. 6E). It showed an apparent saturation after 10 hrs of induction when it amounted to about 250  $\mu mol.l^{-1}$  per 20 min, but a maximum of  $412 \pm 30 \mu mol.l^{-1}$  per 20 mins was observed 15 hrs after induction and with 10  $mmol.l^{-1}$  of  $[Mg^{2+}]_e$ . The  $[Mg^{2+}]_i$  increase observed under the latter conditions showed strong temperature sensitivity. In the experiments summarized in figure 7A, media temperatures were held at 37°C (control), 25°C or 40°C during the 20-mins measurement period. Reduction or elevation of the temperature significantly decreased ( $0.33 \pm 0.03 mmol.l^{-1}$ ) or increased ( $1.29 \pm 0.06 mmol.l^{-1}$ ) the end point  $[Mg^{2+}]_i$  of SLC41A1 over-expressing cells when compared with that ( $0.95 \pm 0.03 mmol.l^{-1}$ ) observed in control cells. This corresponded to changes in the apparent  $Mg^{2+}$  accumulation that amounted to  $569 \pm 20$ ,  $79 \pm 7$  and  $737 \pm 54 \mu mol.l^{-1}$  when cells were measured under control, low- or high-temperature conditions, respectively (fig. 7A).

Next, we wished to determine whether the observed  $[Mg^{2+}]_i$  changes were accompanied by net changes of  $[Mg]_i$  (measured by AMS). In these experiments, all cells were pre-starved in  $Mg^{2+}$ -free medium for 60 mins (this time was adequate for mag-fura 2 AM loading and activation in the FFS measurements described above) and then incubated in the presence of 10  $mmol.l^{-1}$   $Mg^{2+}$  over a time period of 20 mins. As shown in fig. 7B, the  $[Mg]_i$  of -tet HEK293-(SLC41A1) cells was not influenced by incubation in  $Mg^{2+}$ -free or high- $Mg^{2+}$  (10  $mmol.l^{-1}$ ) medium. However, when +tet (5 hrs) HEK293-(SLC41A1) cells were kept in  $Mg^{2+}$ -free medium, their  $[Mg]_i$  decreased by

25.6% compared to that of -tet cells incubated under the same conditions. Again, such results are only explainable by an increased SLC41A1-mediated  $Mg^{2+}$  efflux from these cells. When  $Mg^{2+}$  (10  $mmol.l^{-1}$ ) was present during the 20-min incubation time, the  $[Mg]_i$  of these cells increased by +12.7% indicating replenishment of the intracellular  $Mg^{2+}$  stores by another mechanism than SLC41A1. The same results were observed after an extension of the *hSLC41A1* induction period to 15 hrs.

Furthermore, we tested whether extension of the  $Mg^{2+}$ -starvation and/or -loading time would lead to a further decrease and/or increase of  $\Delta[Mg]_i$  in +tet HEK293-(SLC41A1) cells. Increasing the incubation time in 0 mM- $Mg^{2+}$  medium from 20 to 180 mins reduced  $[Mg]_i$  by 15.4% (5 hrs +tet) and 21.7% (15 hrs +tet), respectively. A prolongation of the  $Mg^{2+}$ -loading time, however, resulted in an 32.6% (5 hrs +tet) and 37.9% (15 hrs +tet)  $[Mg]_i$  increase, respectively (fig. 7B).

*Effect of the  $Mg^{2+}$  channel inhibitor cobalt(III)hexaammine on the  $[Mg^{2+}]_i$  of +tet (15 hrs) HEK293-(SLC41A1) cells and on TRPM7-mediated  $Mg^{2+}$  conductance*

To differentiate channel- and carrier-mediated transport components, we next determined whether the only known inhibitor of channel-mediated  $Mg^{2+}$  transport (13; 35) cobalt(III)hexaammine (CoHex) influenced the  $[Mg^{2+}]_i$  of +tet (15 hrs) HEK293-(SLC41A1) cells incubated in media containing 0, 2, 5 or 10  $mmol.l^{-1}$   $MgCl_2$ . No significant effect of 1  $mmol.l^{-1}$  CoHex was seen in  $Mg^{2+}$ -free medium. However, in media with 2, 5 or 10  $mmol.l^{-1}$   $Mg^{2+}$ , the end point  $[Mg^{2+}]_i$  of CoHex-treated cells was reduced by  $134 \pm 8$ ,  $162 \pm 10$  and  $254 \pm 9 \mu mol.l^{-1}$ , respectively, compared with that measured in non-treated control cells. Thus, a CoHex-sensitive component was observable in the presence of extracellular  $Mg^{2+}$  only and amounted to about 25% at each  $[Mg^{2+}]_e$ . Therefore, in another series of experiments, the effects of CoHex on  $[Mg^{2+}]_i$  changes were compared for -tet and +tet (15 hrs) HEK293-(SLC41A1) cells incubated in either totally  $Mg^{2+}$ -free or 10 mM- $Mg^{2+}$  medium (fig. 8A). In -tet cells incubated in 0  $mmol.l^{-1}$   $Mg^{2+}$  medium, CoHex had no significant effect on the  $[Mg^{2+}]_i$  but the inhibitor led to a significant 30% reduction of  $[Mg^{2+}]_i$  in 10  $mmol.l^{-1}$   $Mg^{2+}$  medium (fig. 8A). In

contrast, the SLC41A1-related  $[Mg^{2+}]_i$  change was not influenced by CoHex (Fig. 8A). These data confirm the existence of a CoHex-blockable  $Mg^{2+}$  influx mechanism(s) not identical to SLC41A1 in HEK293 cells. A likely candidate for such a transport mechanism is the TRPM7 ion channel, which is endogenously expressed in this cell type (36). To study the effect of CoHex on TRPM7 current development, we performed patch-clamp experiments in the whole-cell configuration mode with +tet (14-20 hrs) HEK293-(TRPM7) cells (12). CoHex was applied 60 s after the start of the experiment when TRPM7 currents were fully developed. CoHex at 1  $mmol.l^{-1}$  reversibly blocked inward TRPM7 currents (relevant to divalent cations, mainly  $Mg^{2+}$  conductance) by  $51.3 \pm 1.8\%$ , whereas outward TRPM7 currents (relevant to monovalent ion conductance) remained almost unaffected ( $12.3 \pm 0.6\%$  inhibition) in the presence of 2  $mmol.l^{-1}$   $[Mg^{2+}]_e$  (figs. 8B-E).

## Discussion

At present, our understanding of the molecular identity and cellular functions of SLC41A1 is limited. The sequential similarity between SLC41A1 and the putative bacterial  $Mg^{2+}$  transporter MgtE (14) and the upregulation of SLC41A1 expression in response to a low  $Mg^{2+}$  diet (15) lead to the hypothesis that SLC41A1 is involved in  $Mg^{2+}$  homeostasis and/or  $Mg^{2+}$  transport in cells of higher eukaryotes. This hypothesis is supported by our data showing the functional substitution of CorA, MgtA and MgtB  $Mg^{2+}$  transporters by hSLC41A1 in the *Salmonella* strain MM281. Moreover, the results described here provide experimental evidence that SLC41A1, the first molecularly characterized  $Mg^{2+}$  carrier in eukaryotes, probably mediates  $Mg^{2+}$  efflux. The basis for this conclusion is fourfold: (1) over-expression of SLC41A1 in HEK293 cells does not induce detectable  $Mg^{2+}$ -carried currents, (2) in  $Mg^{2+}$ -free media, SLC41A1 over-expression leads to a significant reduction of  $[Mg^{2+}]_i$  and of  $[Mg]_t$ , (3) the intensity of the  $Mg^{2+}$  loss depends on the induction time and thus on the number of SLC41A1 molecules in the cell membrane and (4) SLC41A1-related  $[Mg^{2+}]_i$  changes are temperature-sensitive but not

influenced by the Mg<sup>2+</sup> channel blocker cobalt(III)hexaammine (CoHex).

*hSLC41A1 functionally complements disruption of the CorA-MgtA-MgtB transport system in Salmonella enterica sv. typhimurium*

The Mg<sup>2+</sup>-dependent growth-deficient *Salmonella* strain MM281 represents, with certain limitations, a simple model for testing the ability of the candidate Mg<sup>2+</sup> transporters to restore its growth and thus to identify the direct involvement of these transporters in Mg<sup>2+</sup> transport (24; 37; 38). *SLC41A1* has only been identified in the genomes of eukaryotes (14; 15) however, due to its distant sequential ancestry with the bacterial MgtE, we reasoned that it might be able to complement the growth-deficient phenotype of the MM281 strain. MgtE can mediate Mg<sup>2+</sup> uptake in bacteria but lacks homology to the other known bacterial Mg<sup>2+</sup> transporters as it does not possess the typical F/YGMN motif, which is characteristic for members of the CorA-Mrs2-Alr1 superfamily of Mg<sup>2+</sup> transporters (13). Nevertheless, as our data show, hSLC41A1, when over-expressed from *pUC18-hSLC41A1* in the MM281 strain, partly restores the growth of this triple-disruptant of *Salmonella* in low Mg<sup>2+</sup> media. However, the growth-promoting effect of SLC41A1 is less than that of Mrs2 (13). The latter is present in the mitochondria of the eukaryotes and represents a distant homologue of the bacterial Mg<sup>2+</sup> channel CorA. Functional complementation by SLC41A1 corresponds well to our data obtained by ICP-MS demonstrating a significant increase of the total magnesium concentration in the MM281 strain transformed with *pUC18-hSLC41A1* in comparison with the [Mg]<sub>i</sub> in the MM281 strain transformed with *pUC18-(empty)*. The ability of hSLC41A1 to complement the Mg<sup>2+</sup>-linked growth-deficient phenotype of *Salmonella* strain MM281 identifies hSLC41A1 as being a *bona fide* Mg<sup>2+</sup> transporter.

*hSLC41A1 probably forms hetero-oligomeric complexes in a mammalian expression system*

Taking into account that hSLC41A1 maintains its functionality when expressed in *Salmonella* and that the *Salmonella* genome lacks *mgtE*, hSLC41A1 probably works as a monomer and/or a homo-oligomer in this expression system. However, various solute transporters have been

shown to form stable or transient protein complexes in order to become functional in their native systems (31; 32). This is in agreement with our findings establishing that SLC41A1 forms protein complexes of “high” molecular mass (~1000 kDa) when over-expressed in HEK293 cells. In addition, our 2D-PAGE data indicate the presence of distinct proteins in the observed SLC41A1 complexes, further suggesting the hetero-oligomeric character of SLC41A1 complexes in the mammalian system. SLC41A2 and SLC41A3 are possible candidates for being binding partners in such complexes. This hypothesis is indirectly supported by our recent observation that all three genes are being over-expressed simultaneously in response to extracellular Mg<sup>2+</sup> starvation in lymphocytes (Rolle et al., in prep.). Even so, protein(s) other than SLC41A2 or SLC41A3 (e.g. protein components of the cytoskeleton, other ion transporters and/or enzymes) must be integrated in SLC41A1-containing complexes to reach the observed molecular masses between 720 and 1236 kDa. Future studies investigating SLC41A1-binding partners and the composition of the SLC41A1 complexes in response to specific physiological conditions will clarify this.

*hSLC41A1 over-expression does not induce measurable Mg<sup>2+</sup> currents, but allows Mg<sup>2+</sup> efflux and is associated with an endogenous Cl<sup>-</sup> conductance*

Over-expression of mSLC41A1 in *Xenopus laevis* oocytes has been shown to induce large Mg<sup>2+</sup>-carried currents, although various other divalent cations are also transported (15). Using TEV, Goytain and Quamme (15) determined the following SLC41A1-specific permeation profile: Mg<sup>2+</sup> ≥ Sr<sup>2+</sup> ≥ Fe<sup>2+</sup> ≥ Ba<sup>2+</sup> ≥ Cu<sup>2+</sup> ≥ Zn<sup>2+</sup> ≥ Co<sup>2+</sup> > Cd<sup>2+</sup>. However, because of the lack of a control for the intracellular ion milieu, TEV does not allow the establishment of a true permeation profile. Nevertheless, these data suggest that SLC41A1 is an unspecific divalent cation channel. In contrast, the currents induced by SLC41A1 over-expression in our +tet HEK293-(SLC41A1) cells have been identified as endogenous Cl<sup>-</sup> currents, recruited by depletion of intracellular Mg<sup>2+</sup> and blockable by the broad-spectrum Cl<sup>-</sup> transport antagonist DIDS. These currents are not affected by changing the driving force for Mg<sup>2+</sup> across the plasma

membrane. In accordance with our data, SLC41A2, another member of the SLC41 transporter family, has also been reported to mediate large Mg<sup>2+</sup> currents when expressed in *Xenopus laevis* oocytes (16) but induces no significant currents after expression in TRPM7-deficient DT40 cells (17).

Nevertheless, SLC41A1-related Mg<sup>2+</sup> transport is clearly demonstrated by our results showing changes of the [Mg<sup>2+</sup>]<sub>i</sub> and of the total [Mg] ([Mg]<sub>t</sub>) in +tet HEK293-(SLC41A1) cells. One of the main differences between -tet and +tet HEK293-(SLC41A1) cells is a significantly lower [Mg<sup>2+</sup>]<sub>i</sub> and [Mg]<sub>t</sub> in the latter after incubation in a completely Mg<sup>2+</sup>-free medium ([Mg<sup>2+</sup>]<sub>i</sub> > [Mg<sup>2+</sup>]<sub>e</sub>). This raises the possibility that SLC41A1 mediates Mg<sup>2+</sup> efflux which is supported by the following findings: (1) the intensity of the observed [Mg<sup>2+</sup>]<sub>i</sub> and [Mg]<sub>t</sub> decrease is clearly dependent on the duration of tet-induction and therefore is more pronounced in correlation with the translocation of more SLC41A1 proteins to the cell membrane, and (2) neither wild type (wt) nor -tet HEK293-(SLC41A1) cells ever develop such a significant [Mg<sup>2+</sup>]<sub>i</sub> or [Mg]<sub>t</sub> decrease, even in the absence of extracellular magnesium (table I). In contrast, cells with a low SLC41A1 expression show a slight [Mg<sup>2+</sup>]<sub>i</sub> increase and, as no extracellular Mg<sup>2+</sup> is available under these conditions, the release of the ion from intracellular buffers or organelles might be responsible for this observation. These findings were surprising, because, based on the results of Goytain and Quamme (15), an increased Mg<sup>2+</sup> influx capacity of +tet HEK293-(SLC41A1) was expected. For this reason, our experiments were originally designed to support such SLC41A1-related Mg<sup>2+</sup> uptake by performing all preparation and storage procedures before the actual measurements in Mg<sup>2+</sup>-free solutions. It is very likely that +tet HEK293-(SLC41A1) cells already lose relatively high amounts of intracellular Mg<sup>2+</sup> during this time period due to increased magnesium efflux compared to wild type cells. This assumption is supported by the very low initial [Mg<sup>2+</sup>]<sub>i</sub> levels (~0.2 mmol.l<sup>-1</sup>) measured in +tet HEK293-(SLC41A1) cells incubated in Mg<sup>2+</sup>-free medium.

HEK293 cells express the constitutively active channel TRPM7, which has been shown to mediate Mg<sup>2+</sup> uptake in various cell types (11; 12; 39). Thus, TRPM7 background activity mainly

explains the [Mg<sup>2+</sup>]<sub>i</sub> increase seen in -tet and +tet HEK293-(SLC41A1) cells in the presence of an inwardly directed Mg<sup>2+</sup> gradient. However, a higher efflux capacity after hSLC41A1 over-expression in conjunction with lower initial [Mg<sup>2+</sup>]<sub>i</sub> levels may result in a stronger TRPM7-mediated influx component in +tet HEK293-(SLC41A1) cells. After correction for this component, an apparent “Mg<sup>2+</sup> uptake” still persists resulting in an additional increase of [Mg<sup>2+</sup>]<sub>i</sub> and significantly higher end point [Mg<sup>2+</sup>]<sub>i</sub> levels compared with non-induced control cells. At least at the high [Mg<sup>2+</sup>]<sub>e</sub> of 10 mmol.l<sup>-1</sup>, this is accompanied by a net increase of [Mg]<sub>t</sub>. Although we cannot preclude from the presented results that SLC41A1 can also mediate Mg<sup>2+</sup> influx in the presence of strong inside-directed Mg<sup>2+</sup> gradients, our data suggest a [Mg<sup>2+</sup>]<sub>e</sub>-dependent depression of the SLC41A1 related efflux as the underlying mechanism. Nevertheless, the [Mg<sup>2+</sup>]<sub>i</sub> increase levels off at about 1 mmol.l<sup>-1</sup>, far below the electrochemical equilibrium for Mg<sup>2+</sup> under our experimental conditions. This could be attributable to a negative feedback regulation of TRPM7-mediated Mg<sup>2+</sup> transport or the existence of another unknown Mg<sup>2+</sup> efflux mechanism, such as the Na<sup>+</sup>/Mg<sup>2+</sup> exchanger in HEK293 cells (10).

At a functional level, a DIDS-sensitive anion-linked Mg<sup>2+</sup> efflux system has been described in ventricular heart muscle cells (8). Interestingly, abundant levels of the SLC41A1 transcript has been found in the heart (14) and, together with our data, this makes the protein a good candidate for being the proposed efflux pathway. The failure of H<sub>2</sub>-DIDS to change [Mg<sup>2+</sup>]<sub>i</sub> in our study does not exclude this possibility because it could result from complete inhibition of SLC41A1-related Mg<sup>2+</sup> transport by the unphysiologically high extracellular [Mg<sup>2+</sup>]<sub>e</sub> of 10 mmol.l<sup>-1</sup> used in our experiments. Low-affinity (K<sub>m</sub> for [Mg<sup>2+</sup>]<sub>e</sub> about 2 to 6 mmol.l<sup>-1</sup>), slow and anion-linked (mostly HCO<sub>3</sub><sup>-</sup> and Cl<sup>-</sup>) Mg<sup>2+</sup> transporters also have been functionally described in the basolateral membrane of enterocytes (40; 41), in erythrocytes (42) and ruminal epithelial cells (43).

In some studies (42), Na<sup>+</sup>-independent Mg<sup>2+</sup> efflux was accompanied by channel-mediated and, therefore, separate Cl<sup>-</sup> efflux. This corresponds to our data showing that SLC41A1-related DIDS-blockable Cl<sup>-</sup> conductance and [Mg<sup>2+</sup>]<sub>i</sub> changes in +tet HEK293-(SLC41A1) cells are not directly

linked. Rather, as described in other studies, endogenous Cl<sup>-</sup> channels are activated simply by the reduction of intracellular Mg<sup>2+</sup>, a condition that would also favour Mg<sup>2+</sup> transport by TRPM7. An investigation of the functional role of the observed Cl<sup>-</sup> conductance was beyond the scope of this study. However, the free intracellular [Mg<sup>2+</sup>] is known to be an important regulator of various ion channels, e.g. K<sup>+</sup> and Na<sup>+</sup> channels, with very different functions depending on the cell type. Activation of SLC41A1-related Mg<sup>2+</sup> efflux by at present unknown mechanisms can thus play a special role in such processes.

Cobalt(III)hexaammine (CoHex) is the only known Mg<sup>2+</sup> channel inhibitor showing significant blocking effects on Mg<sup>2+</sup> transport conducted by the bacterial CorA and the mitochondrial Mrs2 channels (13; 35; 44). Here, we demonstrate that CoHex significantly (app. 50%) and reversibly inhibits the Mg<sup>2+</sup>-conductance of the TRPM7 ion channels while leaving SLC41A1-mediated [Mg<sup>2+</sup>]<sub>i</sub> change unaffected. Hence, CoHex may prove to interfere with channel-based Mg<sup>2+</sup> transport mechanisms but not carrier-based mechanisms, increasing the possibilities of identifying distinct Mg<sup>2+</sup> transport mechanisms in various cell systems. Moreover these results give some indication that SLCA1 functions as an Mg<sup>2+</sup> carrier rather than as a channel. An additional feature functionally pointing to a carrier mechanism is the temperature sensitivity of the SLCA1-related Mg<sup>2+</sup> change. Wolf et al. (45) have found a similar 80% reduction of Na<sup>+</sup>/Mg<sup>2+</sup> exchanger activity after a temperature reduction from 37°C to 15-18°C, although the same temperature change has no significant effect on Mg<sup>2+</sup> uptake by the mitochondrial Mg<sup>2+</sup> channel Mrs2 (13).

Goytain and Quamme (15) observed Mg<sup>2+</sup> currents after over-expression of mouse SLC41A1 in *Xenopus* oocytes. This, in contrast to our data,

points to a channel-like behaviour of mouse SLC41A1. Some possible explanation for these diverse results should be given here. One explanation is the simple assumption that, during evolution, the hSLC41A1 Mg<sup>2+</sup> carrier evolved from the mouse SLC41A1 ion channel. SLC41A1 from mouse and human are sequentially almost identical (92% identity and 92% similarity, BlastP version 2.2.9; mSLC41A1 prot. sequence Q8BJA3/NCBI was blasted against hSLC41A1 prot. sequence NP776253/NCBI); thus, on the basis of “structures predetermine functions”, they could transport Mg<sup>2+</sup> in a similar manner. However, this assumption can be easily refuted by considering that certain point mutation(s) can alter not only the ion specificity of the transporter(s) but also the mechanism(s) of the ion transport itself (46; 47; 48).

Another explanation for the above-mentioned difference might be that interactions between SLC41A1 and its binding partners keep the protein functioning as a Mg<sup>2+</sup> carrier in mammalian cells, whereas when it is over-expressed in *Xenopus* oocytes, *Salmonella* or any other non-mammalian expression system, the quantitative and/or qualitative lack of such binding partners result in SLC41A1 functioning as an ion channel. This hypothesis is also supported by the finding that Mg<sup>2+</sup> accumulation observed after the over-expression of *hSLC41A1* in *Salmonella* occurs rapidly and resembles the kinetics of Mg<sup>2+</sup> transport conducted via the CorA channel (Sponder and Kolisek, in prep.; 27). Although we favour this explanation over the first, further experimental investigation will be necessary to describe its molecular basis.

In conclusion, our results show that hSLC41A1 represents a functionally active Mg<sup>2+</sup> carrier mediating Mg<sup>2+</sup> efflux in mammalian cell systems.

## References

1. Cowan, J.A. (2002) *Bio Metals* **15**, 225-35
2. Hartwig, A. (2001) *Mutation Res* **475**, 113-21
3. Bara, M., and Guiet-Bara, A. (2001) *Magnesium Res* **14**, 11-18
4. Kisters, K., Tokmak, F., Kosch, M., Dietl, K.H., and Westermann, G. (1999) *Int J Angiol* **8**, 154-6
5. Saris N.E.L., Mervaala, E., Karppanen, H., Khawaja, J.A., and Lewenstam, A. (2000) *Clin. Chim. Acta* **294**, 1-26
6. Barbagallo, M., Dominguez, L.J., Brucato, V., Galioto, A., Pineo, A., Ferlisi, A., Tranchino, E., Belvedere, M., Putignano, E., and Costanza, G. (2007) In *New perspectives in magnesium research* (Nishizawa, Y., Morii, H., Durlach, J., eds) pp. 213-23, Springer-Verlag, London
7. Quamme, G.A., and Rabkin, S.W. (1990) *Biochem. Biophys. Res. Commun* **167**, 1406-12
8. Ödholm, M.P., and Handy, R.D. (1999) *Biochem. Biophys. Res. Comm* **264**, 334-7
9. Schweigel, M., Vormann, J., and Martens, H. (2000) *Am. J. Physiol. Gastrointest. Liver Physiol* **278**, G400-G408
10. Schweigel, M., Park, H.S., Etschmann, B., and Martens, H. (2006) *Am J Physiol Gastrointest Liver Physiol* **290**, G56-G65
11. Chubanov, V., Gudermann, T., and Schlingmann, K.P. (2005) *Pflugers Arch* **451**, 228-34
12. Schmitz, C., Perraud, A.L., Johnson, C.O., Inabe, K., Smith, M.K., Penner, R., Kurosaki, T., Fleig, A., and Scharenberg, A.M. (2003) *Cell* **114**, 191-200
13. Kolisek, M., Zsurka, G., Samaj, J., Weghuber, J., Schweyen, R.J., and Schweigel, M. (2003) *EMBO J* **22**, 1235-44
14. Wabakken, T., Rian, E., Kveine, M., and Aasheim, H.C. (2003) *Biochem Biophys Res Commun* **306**, 718-24
15. Goytain, A., and Quamme, G.A. (2005) *Physiol Genomics* **21**, 337-42
16. Goytain, A., and Quamme, G.A. (2005) *Biochem Biophys Res Commun* **330**, 701-5
17. Sahni, J., Nelson, B., and Scharenberg, A.M. (2006) *Biochem J* **401**, 505-13
18. Wang, C.Y., Shi, J.D., Yang, P., Kumar, P.G., Li, Q.Z., Run, Q.S., Su, Y.C., Scott, H.S., Kao, K.J., and She, J.X. (2004) *Gene* **306**, 37-44
19. Goytain, A., and Quamme, G.A. (2005) *Physiol Genomics* **22**, 382-9
20. Goytain, A., and Quamme, G.A. (2005) *BMC Genomics* **6**, 48
21. Goytain, A., Hines, R., El-Husseini, A., and Quamme, G.A. (2006) *J Biol Chem Epub*.
22. Hediger, M.A., Romero, M.F., Peng, J.B., Rolfs, A., Takanaga, H., and Bruford, E.A. (2004) *Pflügers Arch. – Eur. J. Physiol* **447**, 465-8
23. Townsend, D.E., Esenwine, A.J., George, J. 3<sup>rd</sup>, Bross, D., Maguire, M.E., and Smith, R.L. (1995) *J Bacteriol* **177**, 5350-4
24. Smith, R.L., Thompson, L.J., and Maguire, M.E. (1995) *J Bacteriol* **177**, 1233-8
25. Bullas, L.R., and Ryu, J.I. (1983) *J Bacteriol* **156**, 471-4
26. Nelson, D.L., Kennedy, E.P. (1971) *J. Biol. Chem* **246**, 3042-9
27. Froschauer, E.M., Kolisek, M., Dietrich, F., Schweigel, M., and Schweyen, R.J. (2004) *FEMS Microbiology Letters* **237**, 49–55
28. Swamy, M., Siegers, G.M., Minguet, S., Wollscheid, B., and Schamel, W.A. (2006) *Sci STKE* **345**, 14
29. Gryniewicz, G., Poenie, M., and Tsien, R.Y. (1985) *J Biol Chem* **260**, 3440-50
30. Jin, L., Amaya-Mazo, X., Apel, M.E., Sankisa, S.S., Johnson, E., Zbyszynska, M.A., Han, A. (2007) *Biophys Chem* **128**, 185-96
31. Urbanowski, J.L., and Piper, R.C. (1999) *J Biol Chem* **274**, 38061-70
32. Chubanov, V., Waldegger, S., Mederos y Schnitzler, M., Vitzthum, H., Sassen, M.C., Seyberth, H.W., Konrad, M., and Gudermann, T. (2004) *Proc Natl Acad Sci U S A* **101**, 2894-9

33. Reddy, M.M., and Quinton, P.M. (1994) *J Membr Biol* **140**, 57-67
34. Meyer, K., and Korbmacher, C. (1996) *J Gen Physiol* **108**, 177-93
35. Kucharski, L.M., Lubbe, W.J., and Maguire, M.E. (2000) *J Biol Chem* **275**, 16767-73
36. Nadler, M.J., Hermosura, M.C., Inabe, K., Perraud, A.L., Zhu, Q., Stokes, A.J., Kurosaki, T., Kinet, J.P., Penner, R., Scharenberg, A.M., and Fleig, A. (2001) *Nature* **41**, 590-5
37. Hmiel, S.P., Snively, M.D., Florer, J.B., Maguire, M.E., Miller, C.G. (1989) *J Bacteriol* **171**, 4742-51
38. Smith, R.L., Gottlieb, E., Kucharski, L.M., and Maguire, M.E. (1998) *J. Bacteriol* **180**, 2788-91
39. He, Y., Yao, G., Savoia, G., and Touyz, R.M. (2005) *Circ. Res* **96**, 207-15
40. Bijvelds, M.J.C., Kolar, Z.I., Wendelaar Bonga, S.E., and Flik, G. (1996) *J. Membrane Biol* **154**, 217-25
41. Jüttner, R., and Ebel, H. (1999) *Biochem Biophys. Acta* **1370**, 51-63
42. Günther, T., and Vormann, J. (1995) *Biochim Biophys Acta* **1234**, 105 –10
43. Schweigel, M., and Martens, H. (2003) *Am J Physiol Gastrointest Liver Physiol* **285**, G45-G53
44. Snively, M.D., Florer, J.B., Miller, C.G., and Maguire, M.E. (1989) *J. Bacteriol.* **171**, 4761-6
45. Wolf, F.I., Di Francesco, A., Covacci, V., and Cittadini, A. (1995) In *Advances in magnesium research* (Smetana, R., ed) Suppl. 1 (1997) to *Magnesium Research* 490-6
46. Gunthorpe, M.J., and Lummis, S.C. (2001) *J Biol Chem* **276**, 10977-83
47. Gadsby, D.C. (2004) *Nature* **427**, 795-7
48. Scheel, O., Ydebik, A.A., Lourdel, S., and Jentsch, T.J. (2005) *Nature* **436**, 424-7

#### Footnotes

We are grateful to Reinhold Penner (The Queen's Medical Center, Honolulu, USA), Rudolf J. Schweyen (Max F. Perutz Laboratories, Vienna, Austria) and Jean-Pierre Kinet (Beth Israel Deaconess Medical Center, Boston, USA) for helpful criticism, to Hans-Christian Aasheim (Radium Hospital, Oslo, Norway) for sending us the *pGEM-T-hSLC41A1*, to Peter Spindler (ARC Seibersdorf research GmbH, Austria) for assisting us with ICP-MS analyses and to Mahealani Monteilh-Zoller (QMC, Honolulu), Renate Brose (FBN Dummerstorf) and Heike Pröhl (FBN Dummerstorf) for competent technical support. We also thank Dr. Theresa Jones for linguistic corrections. This work was supported by the Free University Berlin and Protina Pharmazeutische GmbH funding to MK, Avenir funding to PL and NIH P01GM078195 to AF.

#### Figure legends

Fig. 1. Expression and cellular localization of FLAG-hSLC41A1 (56 kDa) in HEK293-(FLAG-SLC41A1) cells. (A) The most probable computer-predicted model of SLC41A1 membrane topology. (B) Confocal immuno-localization of FLAG-hSLC41A1, in -tet and +tet (15 hrs) cells. FLAG-SLC41A1 immuno-labeled with primary M2 anti-FLAG and secondary GAM Alexa-488 antibodies (green signal) was detected exclusively in the cytoplasmic membrane of +tet cells. Plasma membranes of both, -tet and +tet cells were fluorescently contrasted with WGA conjugated to Alexa-594 (red signal). The yellow color in the merged image show that both signals colocalize in +tet cells. (C) Immuno-detection of recombinant FLAG-hSLC41A1 in total protein isolate (T), non-membrane protein fraction (N) and membrane protein fraction (M) of -tet and +tet (18 hrs) HEK293-(FLAG-SLC41A1) cells. FLAG-SLC41A1 was immuno-detected with anti-FLAG-HRP antibody or M2 anti-FLAG : GAM-kappa-HRP antibodies. No FLAG-hSLC41A1 was detected in -tet cells. The highest hSLC41A1 abundance was detected in the M fraction of +tet cells. This was confirmed by Western blot analysis performed with FLAG-

hSLC41A1 immuno-precipitated (IP) from T, N and M. In both cases protein samples were resolved by 10% SDS-PAGE; C = isotype control, F = FLAG-tag.

Fig. 2. Complex forming ability of hSLC41A1 in HEK293-(FLAG-SLC41A1) cells. FLAG-SLC41A1 was immuno-detected with M2 anti-FLAG : GAM-HRP antibodies. (A) Gradient BN-PAGE (4-12%) analysis of SLC41A1 complexes. Successively increasing SDS concentration (as indicated) lead to break-down of “high” molecular mass complexes C1 and C2 resulting in appearance of SLC41A1 complexes with “lower” molecular mass (C3, C4) and of monomeric SLC41A1 (M). (B) Presence of SLC41A1 in C1 and C2 complexes verified by 2D-SDS-PAGE followed by immuno-decoration of SLC41A1.

Fig. 3. Over-expression of His-hSLC41A1 (56 kDa) in *Salmonella* strain MM281. His-tagged protein was immuno-detected with 6x His-tag : GAM-HRP antibodies or 6x His-tag : GAM-kappa-HRP antibodies. Bands corresponding to recombinant His-hSLC41A1 immuno-detected in total protein isolate and to His-hSLC41A1 immuno-precipitated from the third (ProteoExtract™), membrane-protein enriched fraction (IP/MBF3) of MM281 bacteria are shown. Expression of His-hSLC41A1 from *pUC18-hSLC41A1* was induced by addition of IPTG at concentrations indicated in the figure. Protein samples were resolved by 12.5% SDS-PAGE.

Fig. 4. Effect of hSLC41A1 over-expression in *Salmonella*. Growth curves of the *Salmonella* strains MM1927, MM281 transformed with *pUC18-(empty)* and MM281 transformed with *pUC18-hSLC41A1* grown in N-minimal medium supplemented with 10 mmol.l<sup>-1</sup> (A), 100 μmol.l<sup>-1</sup> (B) or 10 μmol.l<sup>-1</sup> (C) MgCl<sub>2</sub>. Growth curves averaged from three independent experiments for each respective [Mg<sup>2+</sup>]<sub>e</sub> and corresponding serial dilutions (below) plated on the solid N-minimal medium are shown. (D) Steady-state [Mg<sup>2+</sup>]<sub>i</sub> of bacteria from strains MM1927, MM281 transformed with *pUC18-(empty)* and MM281 transformed with *pUC18-hSLC41A1* measured after a 20-min incubation in nominally Mg<sup>2+</sup>-free or 10 mmol.l<sup>-1</sup> Mg<sup>2+</sup> containing saline. Means ± SE of 3 to 4 independent experiments are given; OD, optical density.

Fig. 5. Electrophysiological characterization of hSLC41A1 related current in HEK293-(SLC41A1) cells (ind., induced; non-ind., non-induced). (A) Average current densities at -80 mV and +80 mV induced by Mg<sup>2+</sup>-free internal saline in +tet (15-18 hrs) and -tet HEK293-(SLC41A1) cells. (B) Examples of current-voltage (I-V) relationships at plateau current in +tet and -tet cells extracted from experiments shown in A. (C) Average current densities at -80 mV and +80 mV induced by Mg<sup>2+</sup>-free internal saline in +tet (15-18 hrs) HEK293-(SLC41A1) cells compared to average current densities induced by internal saline containing 1 mmol.l<sup>-1</sup> Mg<sup>2+</sup> in +tet (15-18 hrs) HEK293-(SLC41A1) cells. (D) Examples of current-voltage (I-V) relationships at plateau current in +tet cells perfused with Mg<sup>2+</sup>-free or 1 mmol.l<sup>-1</sup> Mg<sup>2+</sup> internal solution extracted from experiments shown in C. (E) Average normalized currents at -80 mV and +80 mV induced by Mg<sup>2+</sup>-free internal saline in +tet (15-18 hrs) HEK293-(SLC41A1) cells. From t = 200 to 300 s 115 mmol.l<sup>-1</sup> MgCl<sub>2</sub> was applied externally via an application pipette. Inward and outward currents were normalized to the current size at -80 mV after 200 s (immediately before application of 115 mmol.l<sup>-1</sup> MgCl<sub>2</sub>). (F) Average current densities at -80 mV and +80 mV induced by Mg<sup>2+</sup>-free internal saline in +tet cells. 100 μmol.l<sup>-1</sup> DIDS was applied externally via application pipette from t = 300 to 400 s. (G) Examples of I-V relationships of the current before (at 300 s) and at the end (at 400 s) of a 100 μmol.l<sup>-1</sup> DIDS application. Traces are extracted from experiments shown in D. (H) Average current densities at -80 mV and +80 mV induced by internally applied 1 mmol.l<sup>-1</sup> ATPγS in +tet and -tet cells. (I) Average I-V relationships at plateau current in +tet and -tet cells extracted from experiments shown in F. (J) Average current densities at -80 mV and +80 mV induced by Mg<sup>2+</sup>-free internal saline (buffered with 10 mmol.l<sup>-1</sup> HEDTA)

in the presence of  $100 \mu\text{mol.l}^{-1}$  external DIDS in +tet cells.  $100 \text{ mmol.l}^{-1}$   $MgCl_2$  was applied externally via application pipette from  $t = 100$  to  $200$  s.

Fig. 6. Effect of hSLC41A1 over-expression on the free intracellular  $Mg^{2+}$  concentration ( $[Mg^{2+}]_i$ ) of HEK293 cells. (A) Representative original recordings for  $[Mg^{2+}]_i$  of -tet and +tet (15 hrs) HEK293-(SLC41A1) cells at various  $[Mg^{2+}]_e$  and  $[Ca^{2+}]_e$ . Note the continuous  $[Mg^{2+}]_i$  decrease in +tet HEK293-(SLC41A1) cells during exposure to  $Mg^{2+}$ -free medium. (B) Summary of results showing SLC41A1-dependent reduction of  $[Mg^{2+}]_i$  after incubation of +tet HEK293-(SLC41A1) cells in  $Mg^{2+}$ -free medium. Mean  $[Mg^{2+}]_i$  decrease after 20-mins exposure to completely  $Mg^{2+}$ -free is shown. Values are means  $\pm$  SE of 5 to 8 single experiments.  $*P < 0.05$  vs. -tet cells  $**P < 0.01$  vs. -tet cells. (C) Influence of  $H_2$ -DIDS on  $[Mg^{2+}]_i$  of +tet (15 hrs) HEK293-(SLC41A1) cells. Steady state  $[Mg^{2+}]_i$  values measured 20 mins after suspending cells in solutions containing  $10 \text{ mmol.l}^{-1}$   $Mg^{2+}$  are shown for  $H_2$ -DIDS-treated and control cells. Values are means  $\pm$  SE of 7 single experiments. (D)  $[Mg^{2+}]_i$  changes in -tet HEK293-(SLC41A1) cells exposed to inwardly directed  $Mg^{2+}$  gradients. Mean  $[Mg^{2+}]_i$  changes after 20-mins exposure to solutions containing 2, 5 or  $10 \text{ mmol.l}^{-1}$   $Mg^{2+}$  are shown. Line is fitted to data by linear regression analysis (parameters:  $y_0 = 187.8$ ,  $a = 94.5$ ;  $R^2 = 0.99$ ). Data are given as means  $\pm$  SE of 6 single experiments. (E) SLC41A1-dependent increase of  $[Mg^{2+}]_i$  after exposure of +tet (5, 10 and 15 hrs) HEK293-(SLC41A1) cells to inwardly directed  $Mg^{2+}$  gradients. Mean  $[Mg^{2+}]_i$  changes determined after 20-mins exposure to solutions containing 2, 5 or  $10 \text{ mmol.l}^{-1}$   $Mg^{2+}$  and corrected for the increase observed in parallel measurements with -tet HEK293-(SLC41A1) cells are given. Values are means  $\pm$  SE of 6 single experiments. Within an induction time, means that do not have a common lowercase letter differ,  $P < 0.05$ ; within a  $[Mg^{2+}]_e$ , means that do not have a common uppercase letter differ,  $P < 0.05$ .

Fig.7. (A) Temperature sensitivity of SLC41A1-related  $[Mg^{2+}]_i$  changes in HEK293-(SLC41A1) cells.  $[Mg^{2+}]_i$  changes were measured in +tet (15 hrs) HEK293-(SLC41A1) cells incubated in media containing  $10 \text{ mmol.l}^{-1}$   $Mg^{2+}$ . Medium temperatures were held at 37, 25 or  $40^\circ\text{C}$ .  $[Mg^{2+}]_i$  increases obtained after 20-mins exposure to the respective temperature condition are given. The inset shows representative original  $[Mg^{2+}]_i$  recordings. Values are means  $\pm$  SE of 5 to 7 single experiments.  $**P < 0.01$  vs. control ( $37^\circ\text{C}$ ). (B)  $[Mg]_i$  determined in -tet and +tet (5 hrs and 15 hrs) HEK293-(SLC41A1) cells incubated in  $Mg^{2+}$ -free HEK293 medium and in HEK293 medium supplemented with  $10 \text{ mmol.l}^{-1}$   $Mg^{2+}$ . Sets of  $[Mg]_i$  values determined after 20 and 180 mins incubation at these  $[Mg^{2+}]_e$  are shown. Values are means  $\pm$  SE averaged from 3 independent measurements.

Fig.8. Effects of the  $Mg^{2+}$  channel inhibitor CoHex on SLC41A1 and TRPM7  $Mg^{2+}$  transport. (A) Summary of the CoHex effect on the  $[Mg^{2+}]_i$  of -tet and +tet (15 hrs) HEK293-(SLC41A1) cells incubated in either  $Mg^{2+}$ -free or  $Mg^{2+}$ -containing ( $10 \text{ mmol.l}^{-1}$ ) medium. Mean  $[Mg^{2+}]_i$  changes (-tet cells) and mean  $[Mg^{2+}]_i$  changes corrected as described in legend to figure 5E (+tet cells) are shown. Values are means  $\pm$  SE of 3 single experiments.  $*P < 0.05$  vs. control cells (without CoHex). (B) Average current densities at  $-80$  mV and  $+80$  mV induced by  $Mg^{2+}$ -free ( $+10 \text{ mmol.l}^{-1}$  BAPTA) internal saline in +tet (14-20 hrs) HEK293-(TRPM7).  $1 \text{ mmol.l}^{-1}$  CoHex was applied via an application pipette during time course of 60 s (from 240 to 300 s). (C) Averaged I-V relationships extracted from experiments shown in B at current plateau before (at 240 s) and during (at 300 s) application of  $1 \text{ mmol.l}^{-1}$  CoHex. (D) Average inward current at  $-80$  mV shown in B normalized to the current size immediately before application of  $1 \text{ mmol.l}^{-1}$  CoHex ( $I/I_{in \text{ at } 240 \text{ s}}$ ). (E) Extracted part of the I-Vs depicted in C, showing the  $\sim 50\%$  inhibition of the TRPM7 inward current by  $1 \text{ mmol.l}^{-1}$  CoHex.

Table I: [Mg<sup>2+</sup>]<sub>i</sub> (mmol.l<sup>-1</sup>) of non-induced (-tet) and induced (+tet) HEK293-(SLC41A1) cells and of +tet HEK293 wild type (wt) cells measured at various [Mg<sup>2+</sup>]<sub>e</sub>.

[Mg <sup>2+</sup> ] <sub>e</sub> (mmol.l <sup>-1</sup> )	HEK293-(SLC41A1)				HEK293 (wt)	
	-tet	+tet			+tet	
		5 hours	10 hours	15 hours	10 hours	15 hours
0	0.39 ± 0.03	0.16 ± 0.02**	0.22 ± 0.01*	0.10 ± 0.03*	0.34 ± 0.02	0.38 ± 0.07
2	0.47 ± 0.02	0.49 ± 0.02	0.67 ± 0.05**	0.72 ± 0.03**	0.39 ± 0.06	0.44 ± 0.02
5	0.58 ± 0.02	0.60 ± 0.03	0.96 ± 0.08**	0.99 ± 0.03**	0.47 ± 0.05	0.51 ± 0.02
10	0.73 ± 0.02	0.83 ± 0.03*	0.98 ± 0.15*	1.04 ± 0.08**	0.56 ± 0.11	0.68 ± 0.03

[Mg<sup>2+</sup>]<sub>i</sub> values achieved after 20 mins in the respective medium are given. Data are presented as means ± (SE) of 4 to 15 single experiments.

\**P* < 0.05 vs. control (-tet); \*\**P* < 0.01 vs. control (-tet)

Figure 1.

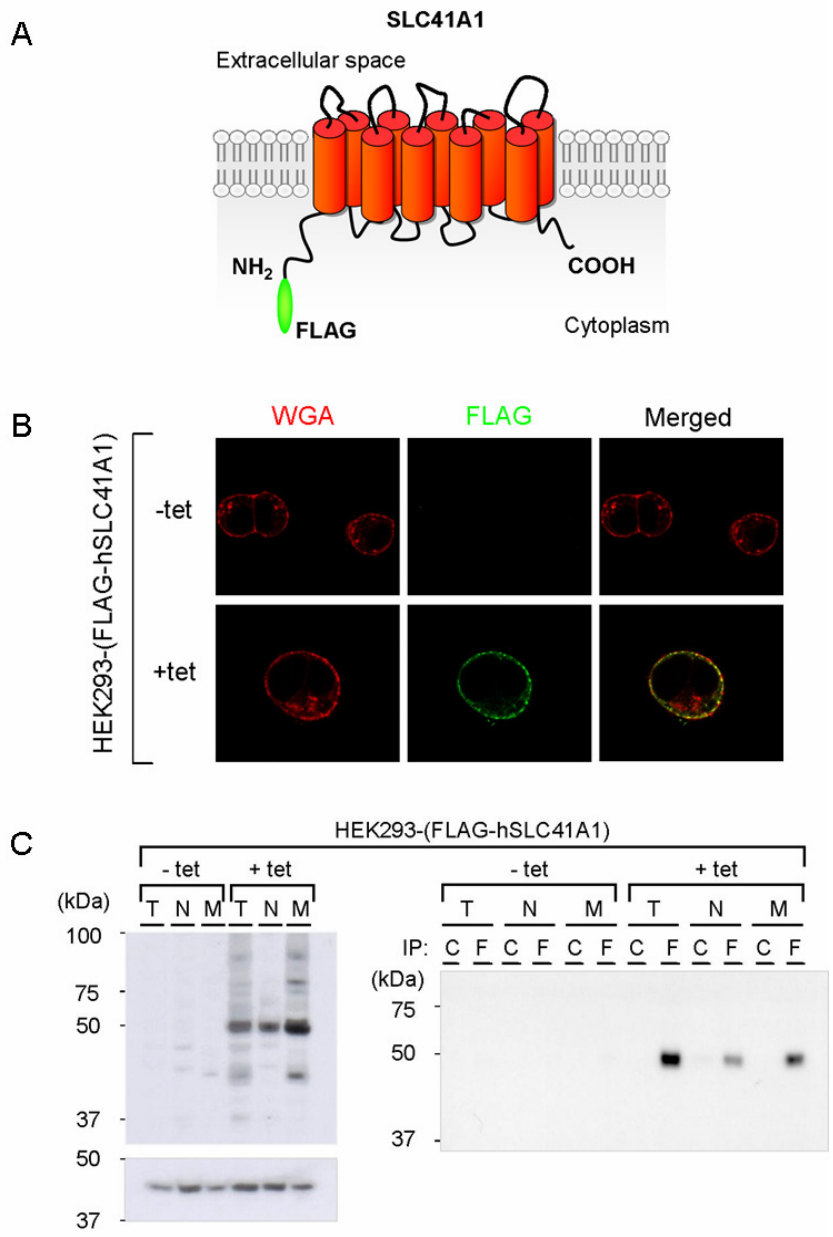


Figure 2.

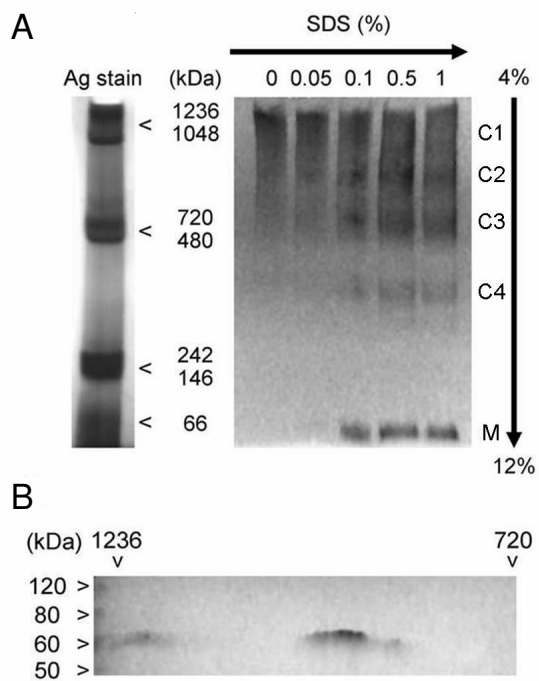


Figure 3.

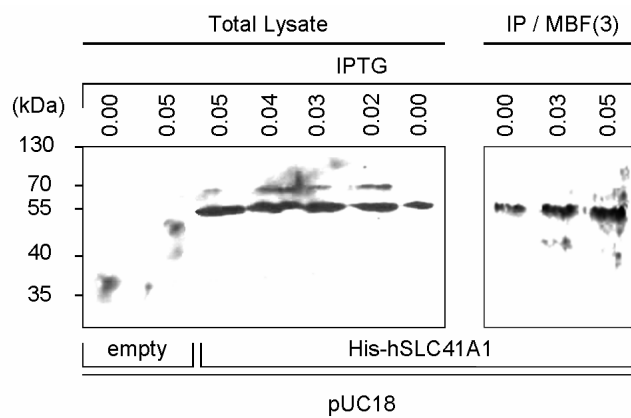


Figure 4.

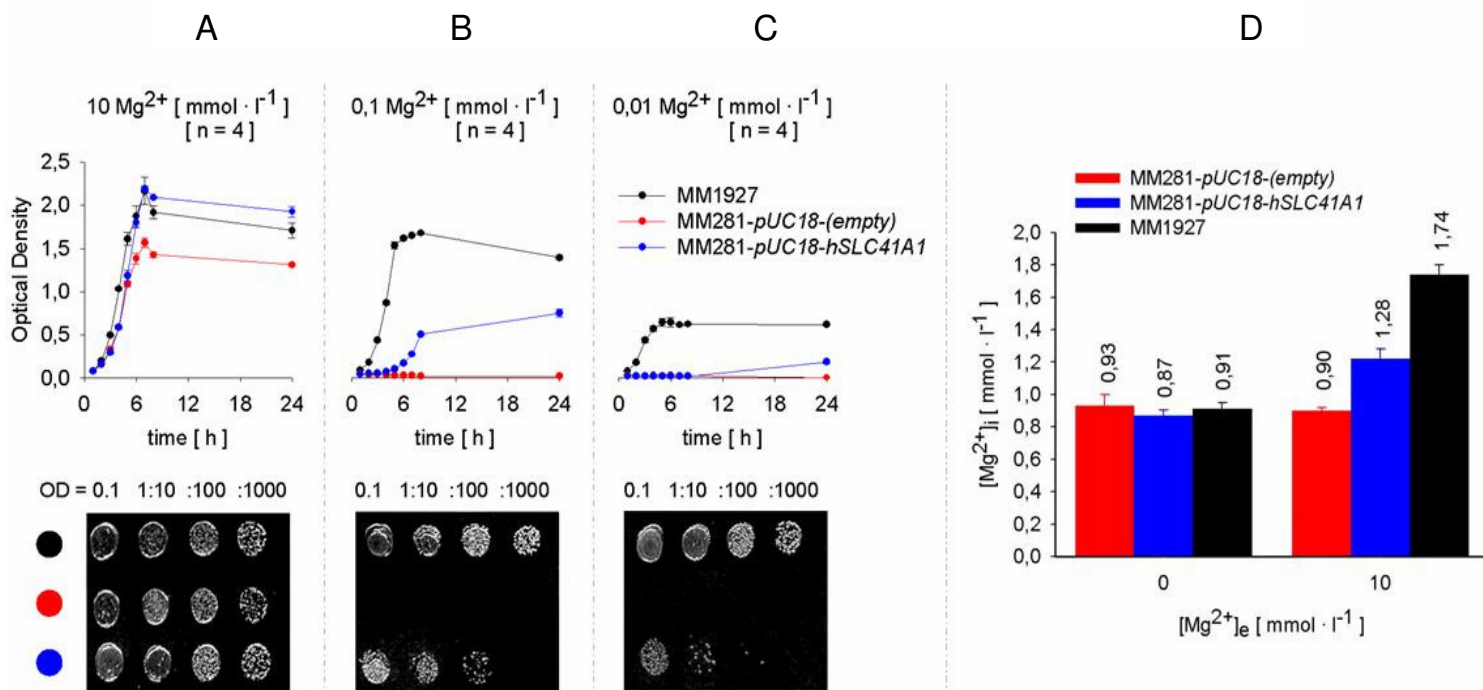


Figure 5.

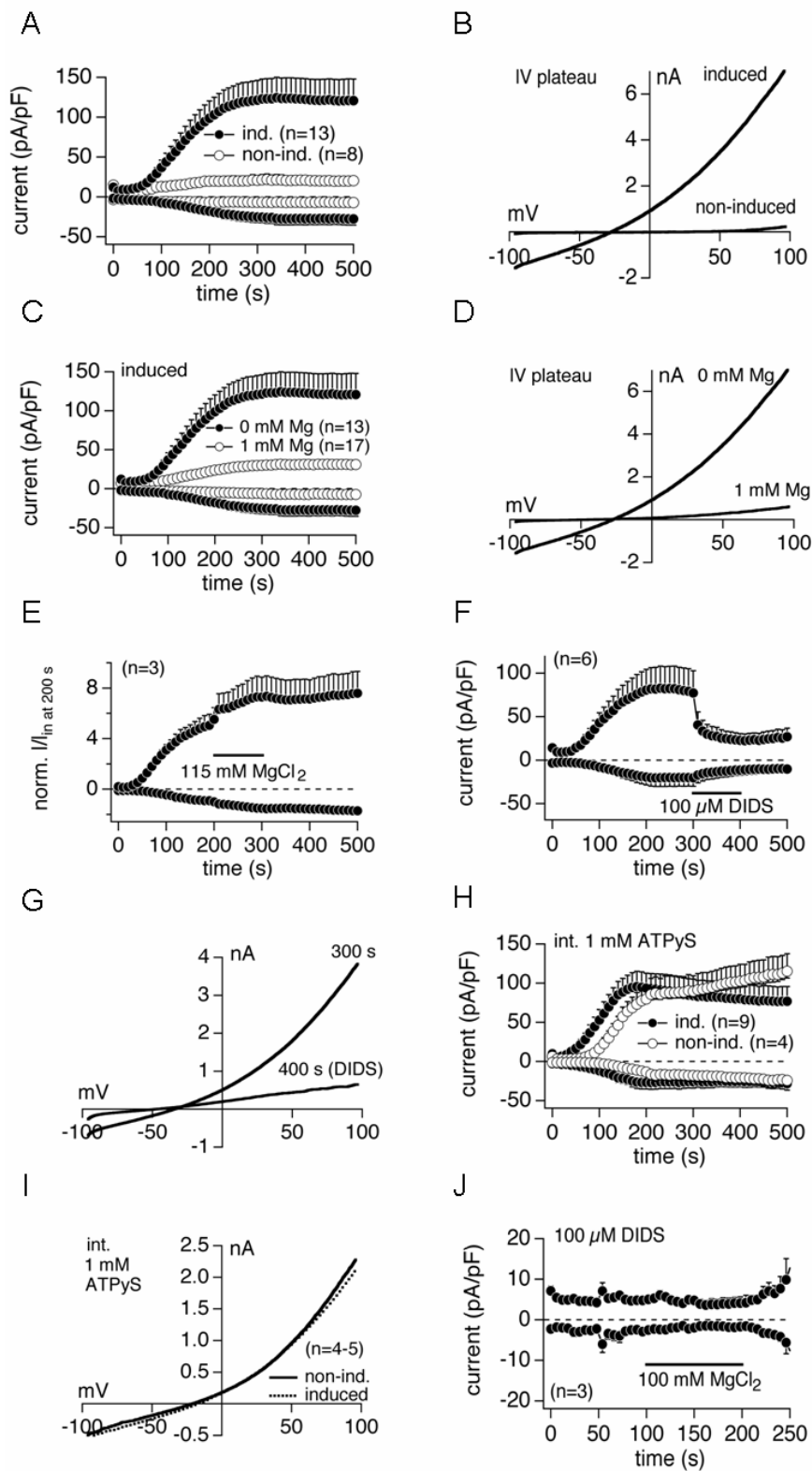


Figure 6.

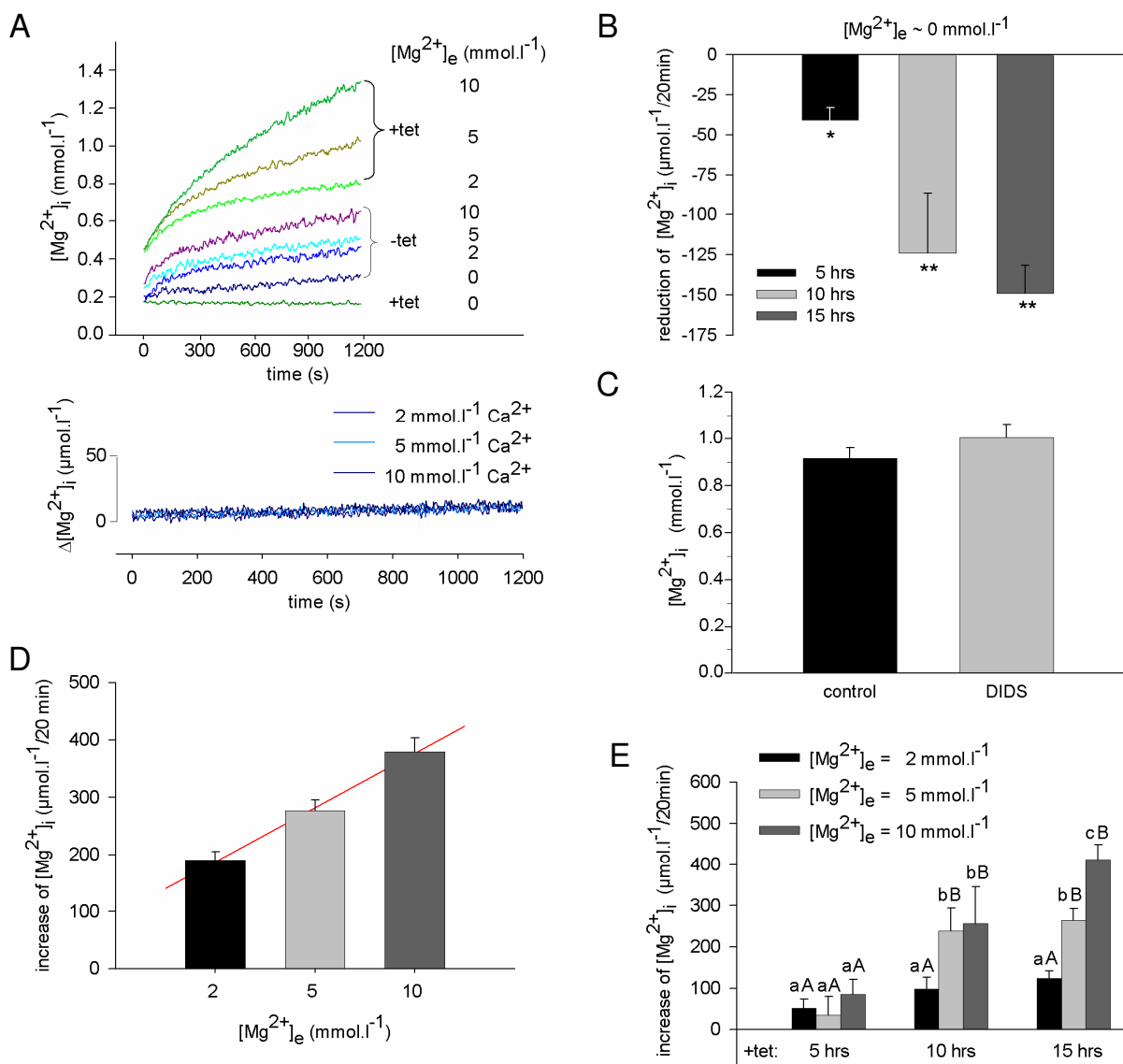


Figure 7.

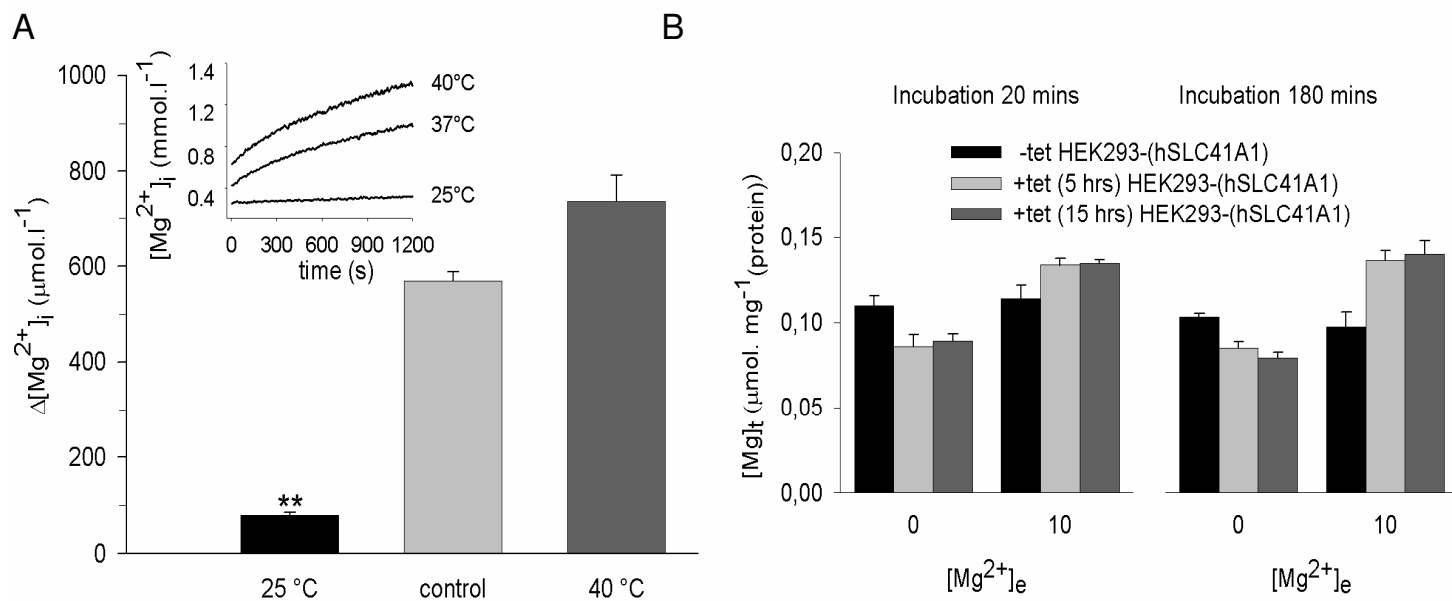


Figure 8.

